the possibility that nuclear-localized 17AA(+)WT1 isoform proteins transcriptionally regulated some molecule(s) that directly acted on mitochondrial membrane and that let the mitochondria stabilize.

Furthermore, to examine whether or not zinc-finger motif (exons 7–10) of the 17AA(+)WT1 isoforms were required for its antiapoptotic functions, polyhistidine-tagged 17AA(+)WT1 protein lacking zinc-finger motif (WT1ΔZF) was stably expressed in K562 leukemia cells (Figure 5a and b). Immunocytochemical analysis showed that polyhistidine-tagged WT1ΔZF protein was detected in the nucleus as full-length WT1 proteins

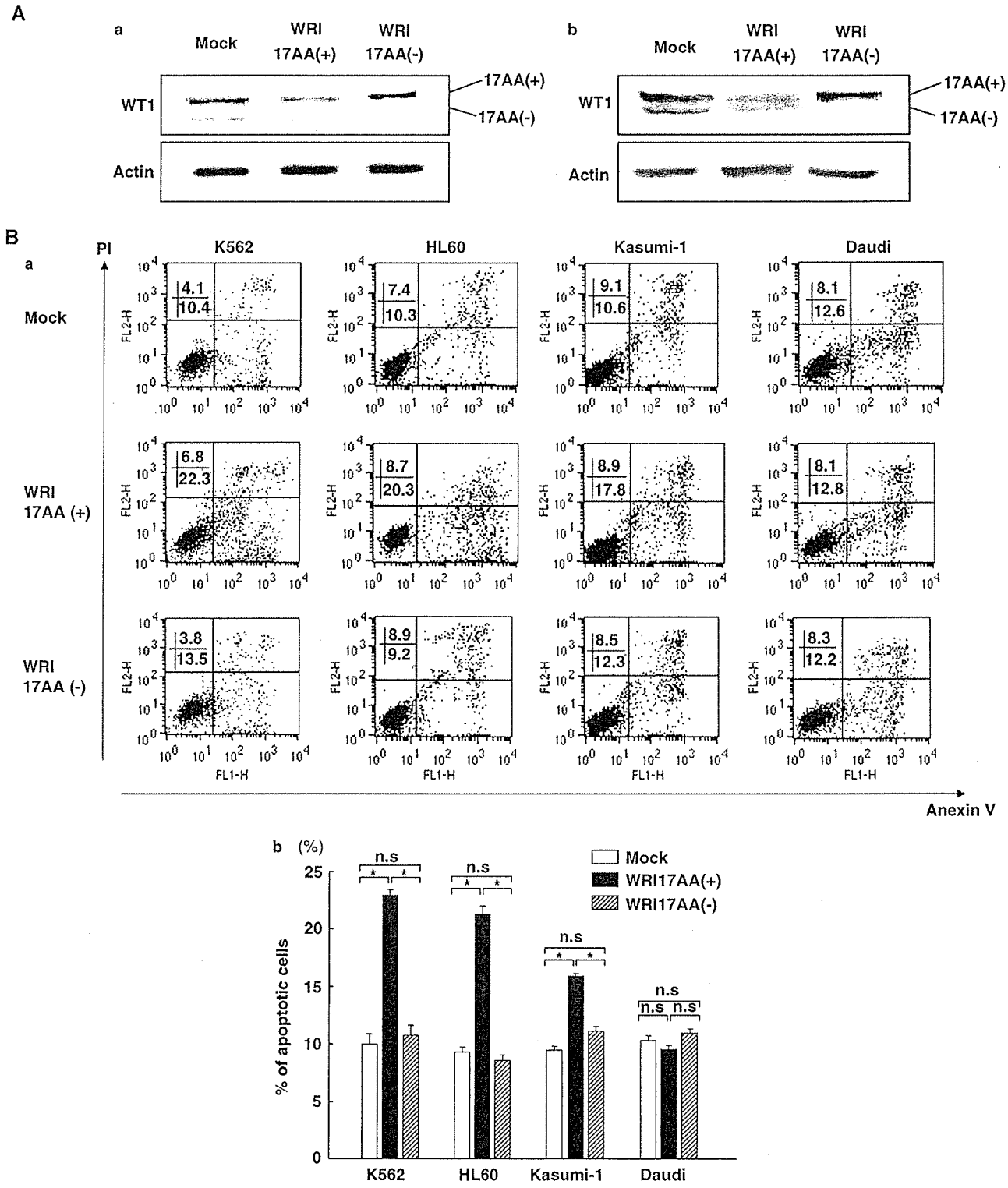


Figure 1 *Continued*

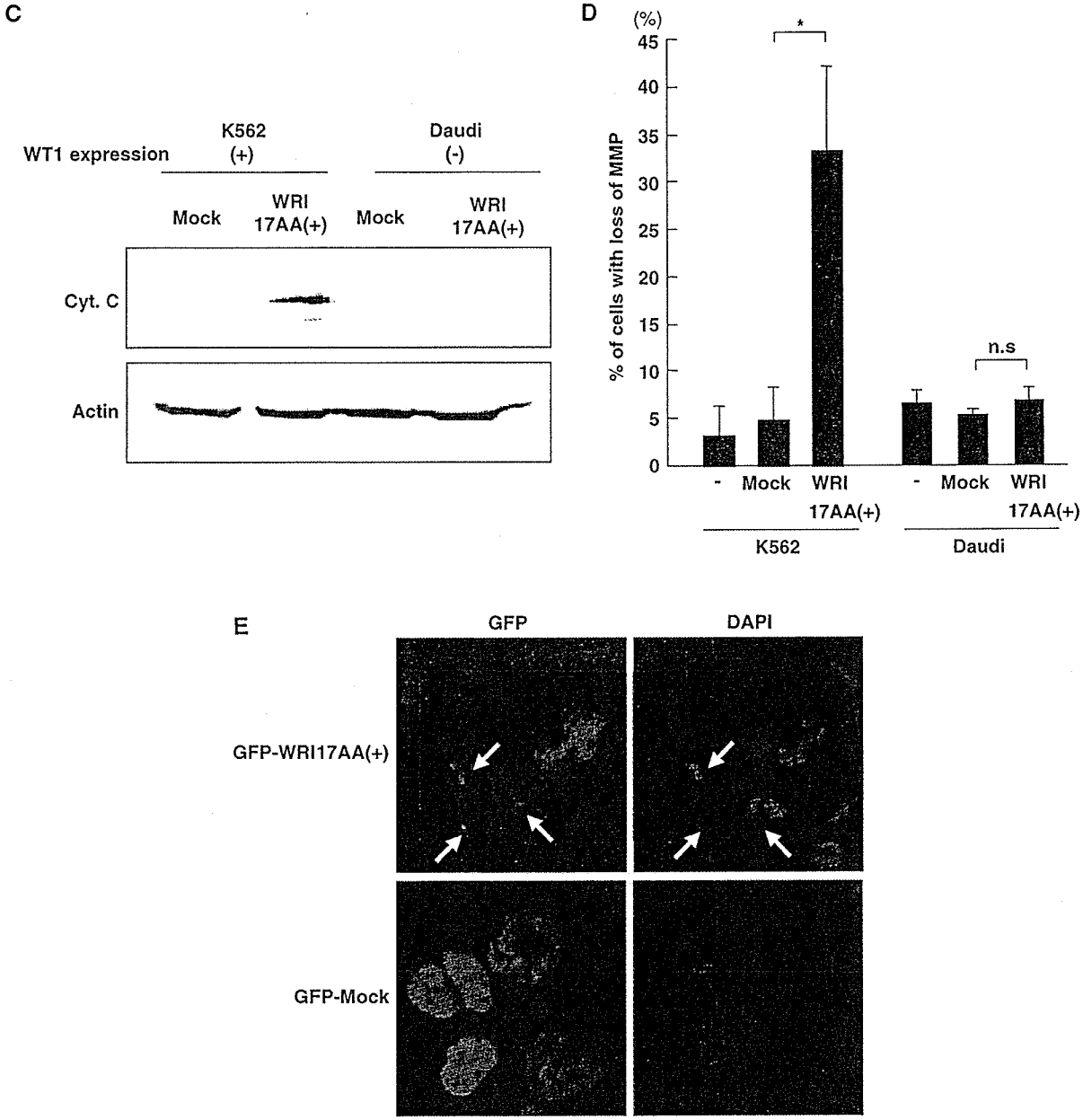


**Figure 1** 17AA(+)WT1-specific siRNA induces apoptosis in WT1-expressing leukemia cells. Three WT1-expressing leukemia cell lines K562, HL-60, and Kasumi-1 and WT1-non-expressing lymphoma cell line Daudi ($2 \times 10^6$ cells) were transfected with 10 $\mu$g of 17AA(+)WT1-specific siRNA vector (WRI17AA(+)), 17AA(−)WT1-specific siRNA vector (WRI17AA(−)), or mock vector by electroporation and incubated for 16 h. Then, cells were collected for analysis. (**A**) Expression of 17AA(+) and 17AA(−)WT1 mRNA and of 17AA(+) and 17AA(−)WT1 protein in K562 cells transfected with 17AA(+)WT1-specific siRNA, 17AA(−)WT1-specific siRNA, or control vector were examined by RT–PCR using a PCR primer pair that jumped WT1 17AA coding sequences (a) and by Western blot analysis using anti-WT1 Ab (6FH2) (b), respectively. Actin was used as an internal control. (**B**) Apoptosis induced by 17AA(+)WT1- or 17AA(−)WT1-specific siRNA was analysed by Annexin V-PI two-color flow cytometry. WRI17AA(+), 17AA(+)WT1-specific siRNA treated; WRI17AA(−), 17AA(−)WT1-specific siRNA treated; Mock, and empty siRNA vector treated. (a) Representative results are shown in dot-plot. (b) Columns, means of percentages of apoptotic (Annexin V + PI−) cells from three independent experiments; bars, s.e. (**C**) Mitochondrial release of cytochrome *c* in K562 and Daudi cells. Representative results of Western blot analysis are shown. (**D**) The loss of MMP was examined by flow cytometry. Columns, means of percentages of cells with loss of MMP from three independent experiments; bars, s.e. (**E**) Specific induction of apoptosis in 17AA(+)WT1-specific siRNA-introduced WT1-expressing cells. K562 cells were transfected with 10 $\mu$g of 17AA(+)WT1-specific siRNA vector or control vector and incubated for 24 h. Representative results of confocal microscopic analysis are shown. Cells transfected with 17AA(+)WT1-specific siRNA vector or control vector were labeled with GFP expression (shown in green). DNA was stained with DAPI (shown in blue). Arrows indicate apoptotic cells.

(Figure 5d). However, stable expression of polyhistidine-tagged WT1ΔZF did not inhibit etoposide-induced apoptosis in K562 cells (Figure 5c). These results indicated that zinc-finger region of 17AA(+)WT1 isoforms was needed to exert its antiapoptotic functions in leukemia cells.

*Expression of proapoptotic Bcl-2 family member Bak was decreased by constitutive expression of 17AA(+)KTS(−)WT1 isoform*

To examine the mechanisms by which 17AA(+)WT1 isoform exerts its antiapoptotic functions, the protein expression levels of a set of known apoptotic-related genes such as CDK inhibitors p21 and p27, proapoptotic Bcl-2 familiy members Bax and Bak, antiapoptotic Bcl-2 family members Bcl-2 and Bcl-XL, and caspase-9 were analysed by Western blot in K562 leukemia cells transduced with one each of four WT1 isoforms. As shown in Figure 6a and b, the expression levels of proapoptotic Bak protein were significantly decreased in 17AA(+)KTS(−)WT1 isoform-transduced K562 cells compared to other three WT1 isoform-transduced ones. On the other hand, expression levels of Bax, Bcl-2, Bcl-XL, p21, p27, and caspase-9 were not different among the four WT1 isoform-transduced K562 cells. These results showed that constitutive expression of 17AA(+)KTS(−)WT1

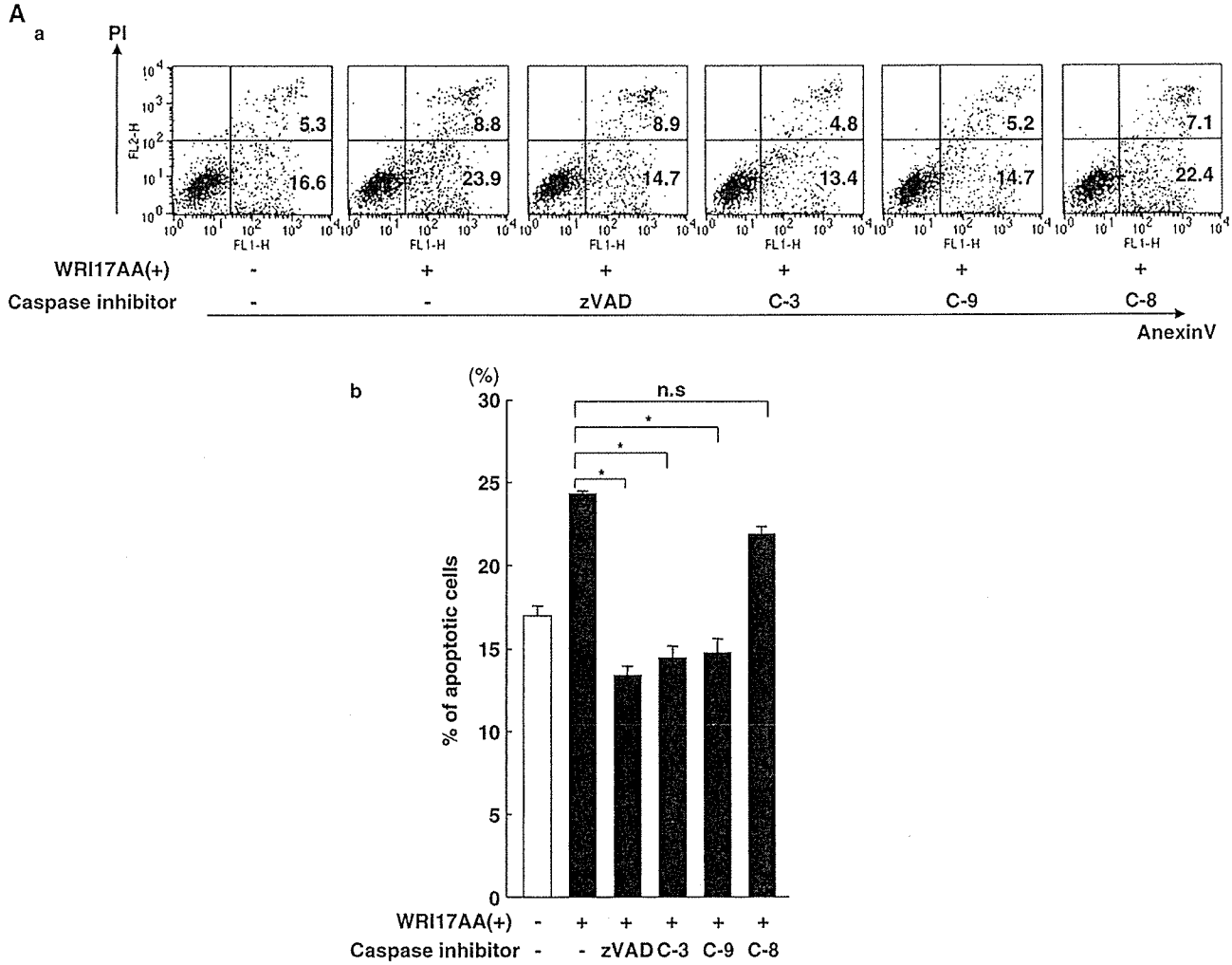


**Figure 2** Transfection of 17AA(+)WT1-specific siRNA activates the intrinsic but not extrinsic apoptosis pathway. (A) K562 cells were transfected with 17AA(+)WT1-specific siRNA vector (WRI17AA(+)) and incubated for 16 h in the presence or absence of broad caspase inhibitor (zVAD-fmk), capsase-3 inhibitor (Ac-DEVD-CHO), capsase-9 inhibitor (Ac-LEHD-CHO), and capsase-8 inhibitor (Ac-IETD-CHO). Then, cells were analysed for apoptosis by Annexin V-PI two-color flowcytometry. zVAD, pan caspase inhibitor zVAD-fmk; C-3, caspase-3-specific inhibitor Ac-DEVD-CHO; C-9, caspase-9-specific inhibitor Ac-LEHD-CHO; and C-8, caspase-8-specific inhibitor Ac-IETD-CHO. (a) Representative results are shown in dot-plots. (b) Columns, means of percentages of apoptotic (Annexin V + PI−) cells from three independent experiments; bars, s.e. $*P<0.05$. (B) Activation of caspases by 17AA(+)WT1-specific siRNA. K562 cells ($2 \times 10^6$ cells) were transfected with 10 $\mu$g of 17AA(+)WT1-specific siRNA vector (WRI17AA(+)), or empty siRNA vector by electroporation, incubated, and collected at the indicated time points. Caspases 3-, 8-, and 9-like activities were measured by fluorometric assay using Ac-DEVD-AFC, FAM-LEHD-FMK, and IETD-pNA, respectively, as substrates. Open column, empty siRNA vector-treated and closed column, 17AA(+)WT1-specific siRNA-treated. zVAD: As a negative control for assays, K562 cells were transfected with WRI17AA(+)-specific siRNA and incubated with broad caspase inhibitor zVAD-fmk (100 $\mu$M) for 24 h. ETP: As a positive control for caspases 3- and 9-like activities, K562 cells were treated with etoposide (100 $\mu$M) for 24 h. TRAIL: As a positive control for caspase-8-like activity, K562 cells were treated with TRAIL (500 ng/ml) for 5 h. Experiments were independently performed three times. bars, s.e. (C) Mitochondrial release of cytochrome *c* by 17AA(+)WT1-specific siRNA. K562 cells were transfected with 17AA(+)WT1-specific siRNA vector (WRI17AA(+)) and incubated for 16 h in the presence or absence of caspase inhibitors. Representative results of Western blot analysis for mithochondrial release of cytochrome *c* are shown. zVAD, pan caspase inhibitor zVAD-fmk; C-3, caspase-3-specific inhibitor Ac-DEVD-CHO; C-9, caspase-9-specific inhibitor Ac-LEHD-CHO; and C-8, caspase-8-specific inhibitor Ac-IETD-CHO. (D) Bax activation by the transfection of 17AA(+)WT1-specific siRNA was examined by Western blot analysis. *, monomer; **, dimer; and ***, oligomer of Bax protein.

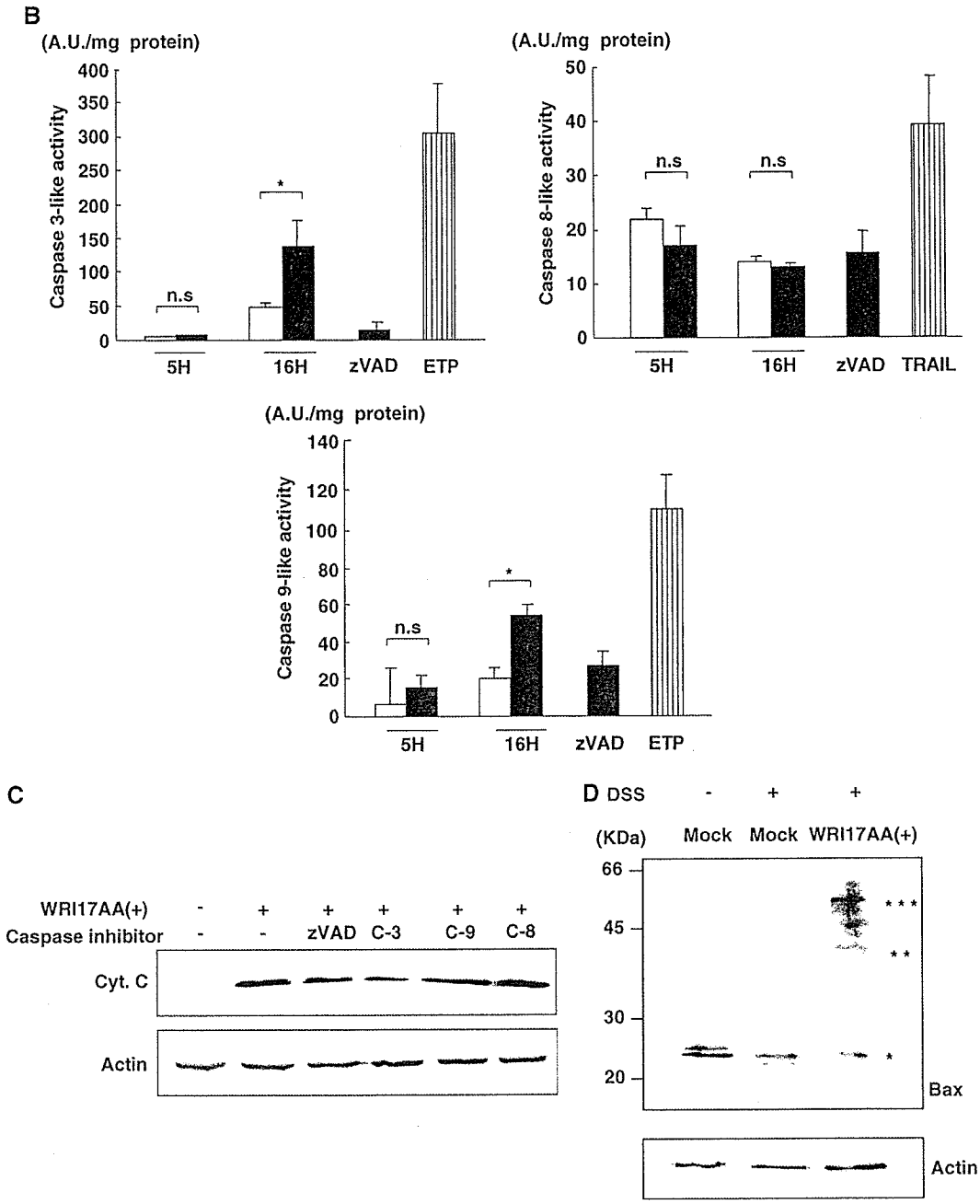


**Figure 2** *Continued*

isoform decreased expression levels of proapoptotic Bcl-2 family member Bak.

## Discussion

Accumulating findings indicate that the *WT1* gene plays oncogenic roles in tumorigenesis of various kinds of cancers. As for the mechanisms by which the *WT1* gene exerts its oncogenic functions, two possible mechanisms, promotion of cell-cycle progression and suppression of apoptosis, may be raised. We and others have reported that suppression of WT1 expression induced G2/M or G1 block in human leukemia K562 cells and HER2/neu-overexpressing breast cancer cells, respectively (Yamagami *et al.*, 1998; Tuna *et al.*, 2005). These results indicated the involvement of the *WT1* gene in cell-cycle progression in cancer cells. Suppression of apoptosis by the *WT1* gene was indicated by the findings that targeted disruption of the *WT1* gene resulted in enhanced apoptosis and embarrassed normal development of organs, including kidney (Kreidberg *et al.*, 1993; Davies *et al.*, 2004), retina (Wagner *et al.*, 2002), and spleen (Herzer *et al.*, 1999) in mice. However, whether or not the *WT1* gene could suppress apoptosis in leukemia cells

and what were precise mechanisms if it had an antiapoptotic function remained unknown. In the present study, we demonstrated a novel oncogenic function of the *WT1* gene to stabilize MMP and to inhibit apoptosis in human leukemia cells and showed that the antiapoptotic function of the *WT1* gene was exerted by 17AA(+)WT1 isoforms (17AA(+)KTS(+) and 17AA(+)KTS(−)) among the four WT1 isoforms. Thus, the *WT1* gene exerted an oncogenic function via both promotion of cell-cycle progression and suppression of apoptosis.

It is important to determine whether or not 17AA(+)WT1 proteins acted at the mitochondria in leukemic cells to understand the mechanism by which 17AA(+)WT1 isoforms block the apoptotic mitochondrial permeabilization. Polyhistidine-tagged 17AA(+)WT1 proteins localized in the nucleus and inhibited etoposide-induced apoptosis. These results raised the possibility that nuclear-localized 17AA(+)WT1 isoform proteins transcriptionally regulated some molecule(s) that directly acted on mitochondrial membrane and let the mitochondria stabilize. This was supported by the findings that proapoptotic Bcl-2 family member Bax, which was activated at a point upstream of the mitochondria, was activated by suppression of expression of 17AA(+)WT1 isoforms in leukemic cells. Therefore, protein expression levels of a set of known apoptosis-related genes such as CDK inhibitors, proapoptotic Bcl-2 family members, antiapoptotic Bcl-2 family members, and caspase-9 were examined in K562 cells transduced with one each of four WT1 isoforms. Expression of proapoptotic Bcl-2 family member Bak was significantly decreased in 17AA(+)KTS(−)WT1 isoform-transduced K562 cells compared to other three WT1 isoform-transduced and control vector-transduced ones (deleted). Since Bak was considered to act as a gateway for various apoptotic signals at the mitochondria, decreased expression of Bak might be one of the mechanisms by which 17AA(+)KTS(−)WT1 isoform exerted its antiapoptotic functions in leukemia cells. As for antiapoptotic Bcl-2 family genes, it was reported that 17AA(+)KTS(−)WT1 isoform functioned as a transcription factor in G401 rhabdoid cells and increased the expression levels of antiapoptotic gene Bcl-2 (Mayo *et al*., 1999). However, both expression levels of Bcl-2 and Bcl-XL in 17AA(+)KTS(−)WT1 isoform-transduced K562 cells were not different from those in control vector-transduced ones.

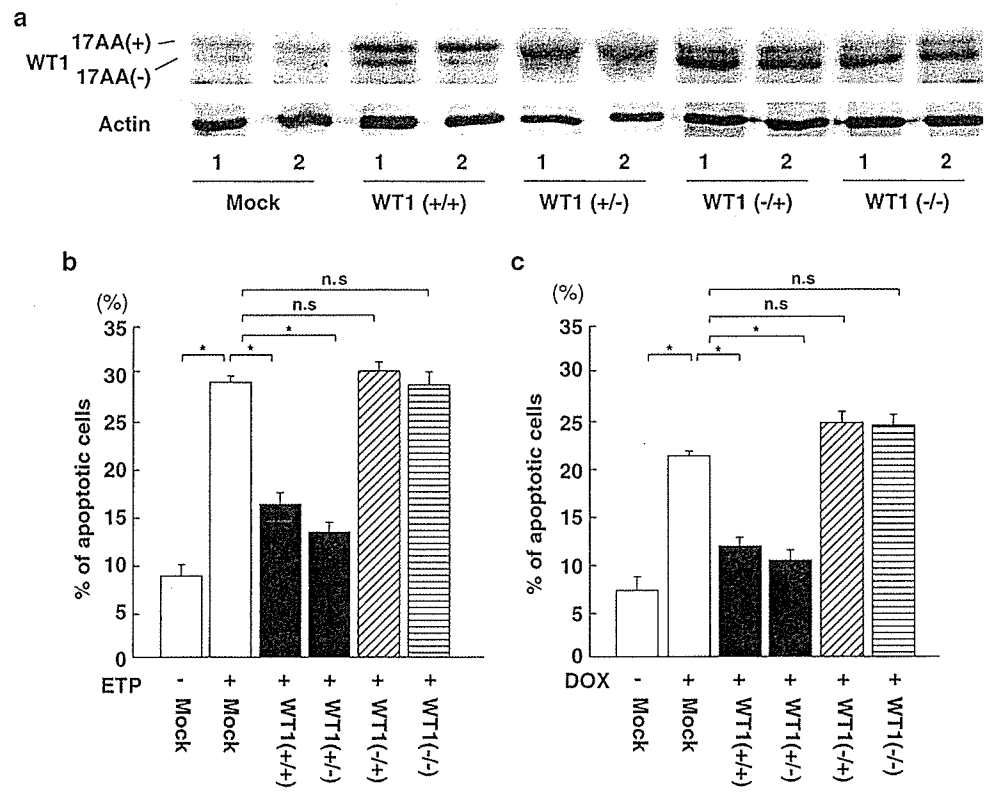


**Figure 3** Stable expression of 17AA(+)WT1 isoforms protects leukemia cells from apoptosis. K562 cell clones that stably expressed one each of four WT1 isoforms at high levels were isolated. The cell clones were treated with etoposide (100 $\mu$M) or doxorubicin (100nM) for 24h. Then, cells were analysed for apoptosis by Annexin V-PI two-color flow cytometric analysis. (**a**) Expression of 17AA(+) and 17AA(−)WT1 proteins in K562 cell clones established. Representative results of Western blot analysis are shown. (**b**, **c**) Apoptosis induced by etoposide (**b**) or doxorubicin (**c**) was analysed by Annexin V-PI two-color flow cytometry. Columns, means of percentages of apoptotic cells in three different K562 cell clones that stably expressed the transduced WT1 isoforms; bars, s.e. Experiments were independently performed three times for each cell clones. (**a**–**c**) WT1(+/+), WT1 17AA(+)KTS(+) isoform; WT1(+/−), WT1 17AA(+)KTS(−) isoform; WT1(−/+), WT1 17AA(−)KTS(+) isoform; and WT1(−/−), WT1 17AA(−)KTS(−) isoform. *$P<0.05$.

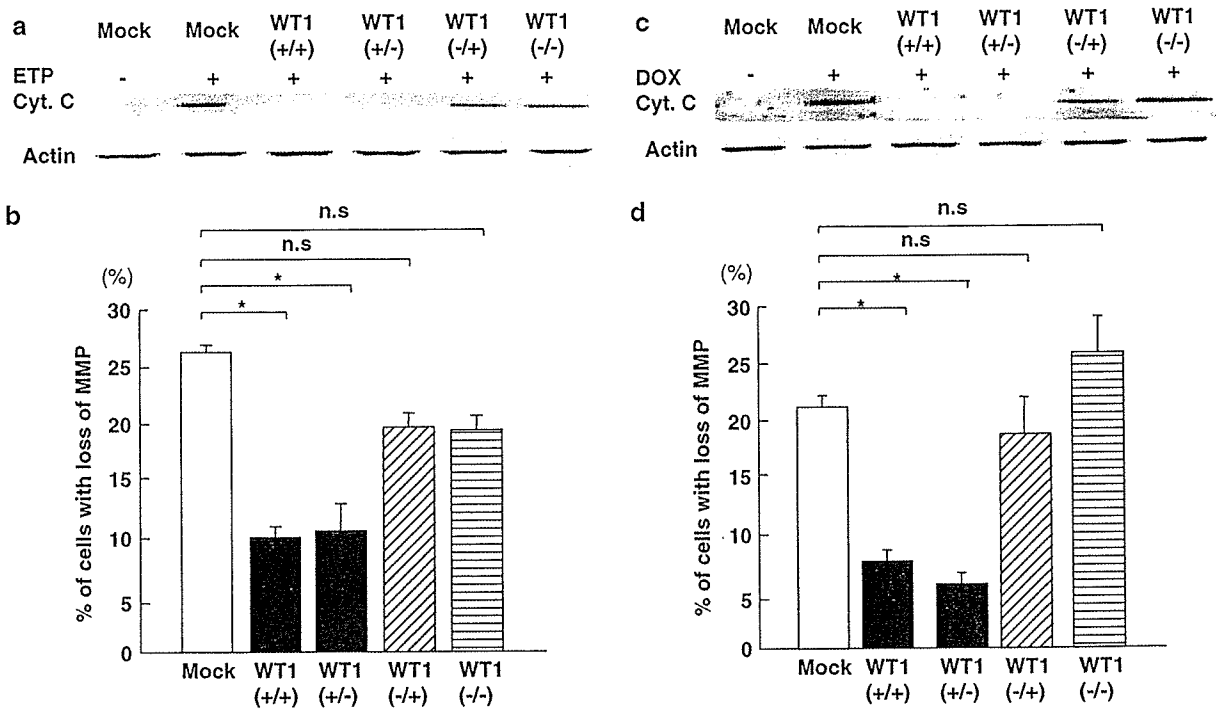


**Figure 4** Stable expression of 17AA(+)WT1 isoforms protects mitochondria from membrane damages induced by apoptosis-inducing drugs. K562 cell clones transduced with one each of four WT1 isoforms were treated with etoposide (100 $\mu$M) or doxorubicin (100nM) for 24 h. Then, mitochondrial damages were examined by Western blot analysis for mitochondrial release of cytochrome *c* and by flow cytometric analysis for loss of mitochondrial membrane potential (MMP). (**a**) Mitochondrial release of cytochrome *c* in K562 clones treated with etoposide. (**b**) Induction of loss of MMP by etoposide. (**c**) Mitochondrial release of cytochrome *c* in K562 clones treated with doxorubicin. (**d**) Induction of loss of MMP by doxorubicin. (**b**) and (**d**) Columns, means of percentages of cells with loss of MMP in three different K562 cell clones that stably expressed the transduced WT1 isoforms; bars, s.e. Experiments were independently performed three times for each cell clones. $*P<0.05$.

In the present study, it was shown that wild-type 17AA(+)WT1 isoforms inhibited apoptosis induced by apoptosis-inducing agents, whereas a mutant 17AA(+)WT1 isoform lacking zinc-finger region (exons 7–10) did not. These results indicated that zinc-finger region was essential for the antiapoptotic functions of 17AA(+)WT1 isoforms. Since zinc-finger region was DNA-binding site of the *WT1* gene, these results indicated that the antiapoptotic function of WT1 17AA(+) isoforms operated through transcriptional regulation of the other genes. As for downstream targets of 17AA(+)WT1 isoforms, proapoptotic Bak might be a direct or indirect target of 17AA(+)KTS(−)WT1 isoform as shown in the present study. As for the downstream target of 17AA(+)KTS(+)WT1 isoform, we could not determine it. However, since this isoform has an insertion of three amino acids (lysine, threonine, and serine (KTS)), by which binding of 17AA(+)KTS(+)WT1 isoform to a consensus sequence as that for 17AA(+)KTS(−)WT1 isoform was abrogated, 17AA(+)KTS(+)WT1 isoform may transcriptionally regulate other gene(s) than one(s) regulated by 17AA(+)KTS(−)WT1 isoforms (Reynolds *et al.*, 2003). Comprehensive studies, including microarray analysis are being planned to identify the targets of 17AA(+)KTS(+)WT1 isoform. Interestingly, both the KTS(+) and KTS(−)WT1 isoforms required 17AA(+) region for their antiapoptotic functions, suggesting the necessity of the interaction with some molecule(s) through this region for their antiapoptotic functions. Taken together, these results may indicate that 17AA(+)KTS(+) and 17AA(+)KTS(−)WT1 isoforms recruit some molecule(s) through the 17AA region, bind to their different target sequences through their zinc-finger regions, and regulate the transcription of target genes to play antiapoptotic roles.

Our data showed that 17AA(+)WT1 isoforms exert antiapoptotic functions in leukemia cells through stabilization of mitochondrial membrane potential. Most chemotherapeutic drugs are considered to initiate cell death primarily by triggering the mitochondrial apoptosis pathway (Shimizu *et al.*, 1996). Constitutive expression of 17AA(+)WT1 isoforms resulted in resistance of K562 leukemic cells to the apoptosis-inducing chemotherapeutic reagent such as etoposide and doxorubicin. Thus, antiapoptotic function of 17AA(+)WT1 isoforms through stabilization of MMP may contribute to chemotherapy resistance in leukemia. Recently, we analysed the expression of the WT1 isoforms in 36 primary leukemias and found that 17AA(+)WT1 isoforms were dominantly expressed in all of these leukemias examined regardless of disease subtypes. Therefore, since suppression of the expression of 17AA(+)WT1 isoforms should improve the sensi-

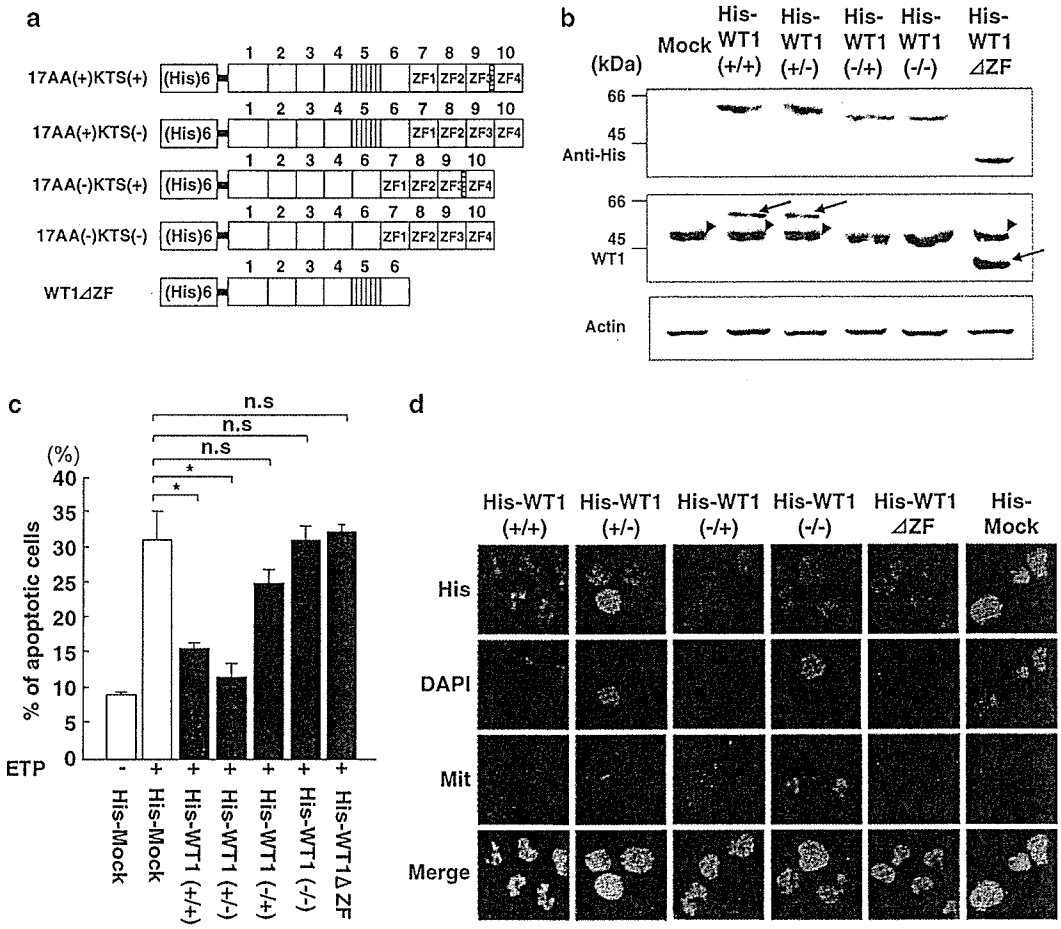


**Figure 5** Requirement of zinc-finger region for the antiapoptotic functions of 17AA(+)WT1 isoforms. Polyhistidine-tagged one each of four WT1 isoforms or 17AA(+)WT1 lacking zinc-finger region (WT1ΔZF) was stably expressed in K562 leukemia cells. (**a**) Construction of four polyhistidine-tagged WT1 isoforms and WT1ΔZF. (**b**) Expression of four polyhistidine-tagged WT1 isoform proteins and WT1ΔZF protein were examined. Representative results of Western blot analysis using anti-polyhistidine tag Xpress (upper), anti-WT1 6F-H2 (middle), and anti-actin (lower) antibodies are shown. In the middle panel, arrows indicate exogeneous polyhistidine-tagged WT1 proteins. Arrowheads indicate endogenous WT1 protein. In polyhistidine tagged-17AA(−)WT1 isoform-transduced cell clones, exogenous polyhistidine-tagged WT1 proteins were not distinguished from endogenous WT1 proteins because molecular weights of these proteins were similar. (**c**) The K562 cell clones were treated with etoposide (100 $\mu$M) for 24 h and analysed for apoptosis by Annexin V-PI two-color flow cytometry. Columns, means of percentages of apoptotic cells in three different K562 cell clones that stably expressed the polyhistidine-tagged WT1 isoforms or WT1ΔZF; bars, s.e. Experiments were independently performed three times for each cell clones. $*P<0.05$. (**d**) Localization of polyhistidine-tagged one each of four WT1 isoforms and WT1ΔZF proteins were examined by immunocytochemistry using anti-His tag Xpress antibody (shown in green). DNA was stained with DAPI (shown in blue). The mitochondria was stained with Mitotracker Red 580 (shown in red).

tivity of leukemia cells to chemotherapeutic drugs, 17AA(+)WT1 isoforms should be a novel molecular target for treatment of leukemia.

## Materials and methods

*Cell lines and culture conditions*

Three highly WT1-expressing leukemia cell lines, chronic myeloid leukemia cell line K562, acute myeloid leukemia cell line Kasumi-1, and acute promyelocytic leukemia cell line HL-60, and one WT1-non-expressing Burkit lymphoma cell line Daudi were cultured in RPMI1640 medium supplemented with 10% fetal bovine serum (FBS).

*Antibodies*

Monoclonal anti-bak (Oncogene Research Products, Boston, MA, USA), anti-WT1 (Dako, Carpinteria, CA, USA), anti-actin (Chemicon, Temecula, CA, USA), anti-Bcl-XL (Chemicon, Temecula, CA, USA), anti-p21 (Oncogene Research Products, Boston, MA, USA), anti-caspase-9 (R&D Systems, Inc., Minneapolis, MN), anti-p27 (BD Biosciences, Pharmingen, San Jose, CA), polyclonal anti-bax (Santa Cruz Biotechnology, Santa Cruz, CA, USA), anti-bcl-2 (Santa Cruz Biotechnology, Santa Cruz, CA, USA), anti-cytochrome *c* (Pharmingen) antibodies, and goat anti-rabbit or anti-mouse IgG conjugated with alkaline phosphatase (Santa Cruz Biotechnology) were used as secondary antibodies in Western blot analysis. For immunocytochemistry, monocolonal anti-His tag (anti-Xpress) (Invitrogen, Carlsbad, CA, USA) and rabbit anti-mouse IgG conjugated with fluorescein isothiocyanate isomer1 (FITC) (DAKO, A/S, Denmark) were used.

*Reagents*

zVAD-fmk (broad-caspase inhibitor), Ac-LEHD-CHO (inhibitor for caspase-9), Ac-DEVD-CHO (inhibitor for caspase-3),

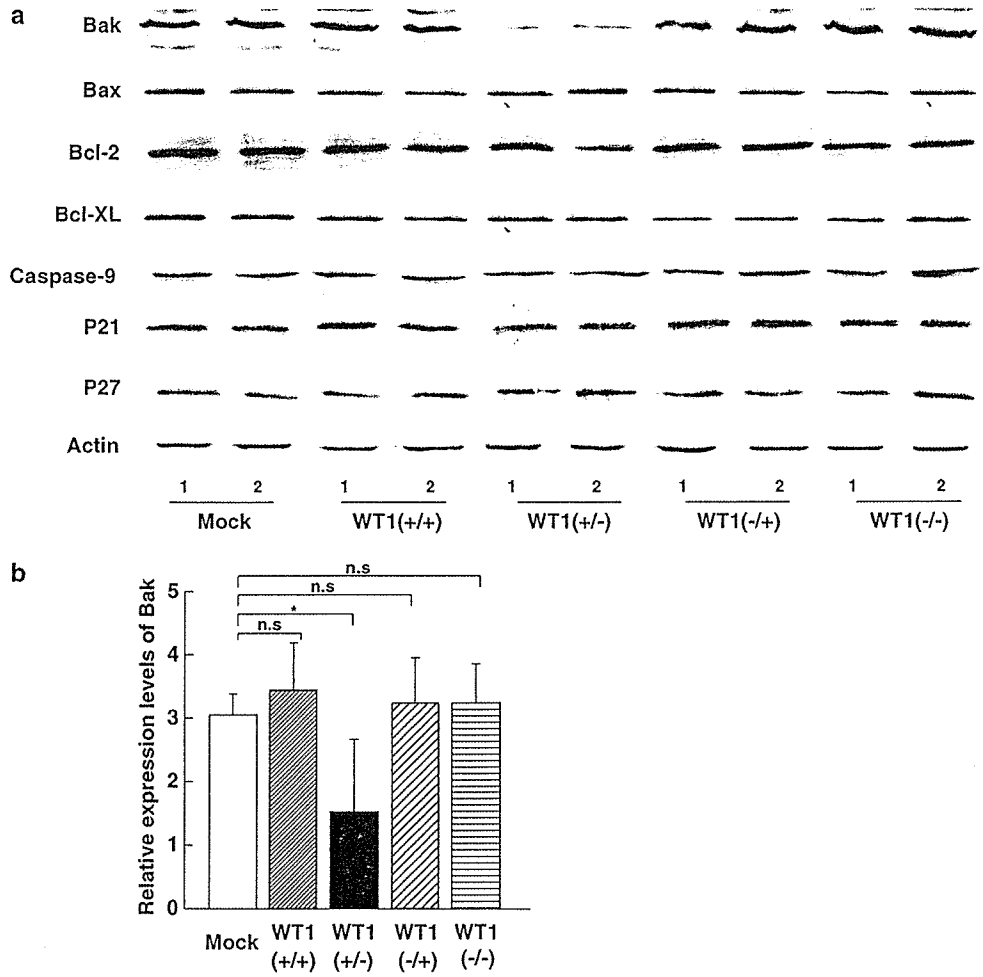


**Figure 6** Expression of apoptotic-related proteins in K562 cell clones transduced with one each of four WT1 isoforms. (**a**) Expression levels of a set of known apoptotic-related proteins in K562 leukemic cells transduced with one each of four WT1 isoforms were examined by Western blot analysis. Three different K562 cell clones transduced with one each of four WT1 isoforms were independently analysed more than two times. Representative results are shown. (**b**) The density of Bak band divided by that of actin band to normalize the difference in protein loading for Western blot analysis in individual samples are shown as relative expression levels. Columns, means of relative expression levels of Bak protein in three different K562 cell clones that stably expressed the transduced WT1 isoforms; bars, s.e. $*P<0.05$.

and Ac-IETD-CHO (inhibitor for caspase-8) (Peptide Institute Inc., Osaka, Japan) were used to inhibit caspase activity at the concentration of 100 $\mu$M. Etoposide (Wako, Osaka, Japan) and Doxorubicin (Sigma Chemical Co., Steinheim, Germany) were used to activate the intrinsic apoptosis pathway and induce apoptosis at the concentration of 100 $\mu$M and 100 nM, respectively. Soluble TRAIL (PEPROTECH EC, London, UK) was used to activate the extrinsic apoptosis pathway and induce apoptosis at the concentration of 500 ng/ml. The enzyme substrate Ac-DEVD-AFC (BIOBOL, Tebu, France), FAM-LEHD-FMK (Serologicals, Norcross, GA, USA), and IETD-pNA (BioVision Lab, Palo Alto, CA, USA) were used to detect caspase-3-like, caspase-9-like, and caspase-8-like activities, respectively. The crosslinkers disuccinimidyl suberate (DSS) (Pierce Biotechnology, Rockford, IL, USA) was used in the detection of dimerization or oligomerization of Bax protein.

*Vector construction*

A pcDNA 3.1(+) (Invitrogen, Carlsbad, CA, USA) containing one each of four human WT1 isoforms (17AA(+)/KTS(+), 17AA(+)/KTS(−), 17AA(−)/KTS(+), and 17AA(−)/KTS(−)) was constructed and used for expression of one each of WT1 isoforms in K562 cells. The sequences of one each of four human WT1 isoforms and WT1 lacking zinc-finger region that were cloned in a pUC119 vector were PCR-amplified using Pfx *Taq* polymerase (Invitrogen, Carlsbad, CA, USA) and integrated into pcDNA 3.1/His vector (Invitrogen, Carlsbad, CA, USA). All the PCR-amplified sequences were confirmed for the absence of mutation by direct sequencing using BigDye Terminator V.1.1 cycle sequencing kit (Applied Biosystem, Branch berg, NJ, USA).

To prepare 17AA(+)WT1- and 17AA(−)WT1-specific siRNA vector, oligonucleotides encoding dsRNA directing (5′-AGCTCCAGCTCAGTGAAATGGACAGAAGGG-3′) in 17AA(+)WT1 mRNA and the sequence corresponding to the ligated sequences flanking the 17AA region in 17AA(−)WT1 mRNA were chemically synthesized, respectively (Japan BioScience, Saitama, Japan), annealed, and inserted into tRNA-shRNA expression vector piGENE tRNA Pur (Clontech, CA, USA) or Gene Silence pGSU6 shRNA Vector (Gene Therapy Systems, Inc., San Diego, CA, USA) which co-expressed GFP.

*Transient expression of siRNA vectors*
For transient transfection of siRNA vectors, K562, HL-60, Kasumi-1, and Daudi cells ($2 \times 10^6$ cells) were washed three times and incubated with 10 $\mu$g plasmid DNA in 300 $\mu$l medium (FBS-) in a 4-mm cuvette. Transfection was performed by electroporation (150 V, 1000 $\mu$F) using Gene Pulser Xcell™ system (BioRad, CA, USA).

*Stable expression of vectors*
Mammalian expression vectors were linealized with *Pvu*I and introduced into K562 cells by electroporation using Gene Pulsor II (BioRad, CA, USA). The cell clones that stably expressed the vectors were isolated using the corresponding selective antibiotics.

*Analysis of apoptosis by flow cytometry*
To assess apoptotic cells, $1 \times 10^5$ cells were washed with PBS, and stained with Annexin V-FITC and PI at room temperature for 15 min in the dark using MEBCYTO Apoptosis Kit (Medical and Biological Laboratories Co., Ltd, Nagoya, Japan) according to the manufacturer's instructions. Then, the stained cells were analysed by FACScan flow cytometer (Becton Dickinson, San Jose, CA, USA). Apoptosis was shown as percentages of apoptotic cells to the total number of counted cells.

*Determination of cytochrome* c *release*
To assess the release of cytochrome *c* from mitochondria to cytoplasm, cells were washed once with PBS, lysed in ice-cold STE buffer (250 mM sucrose, 25 mM Tris, and 1 mM EDTA, pH 6.8), and immediately centrifuged at 15 000 *g* for 15 min. The supernatants were mixed with an equal volume of 2 × Laemmeli's SDS sample buffer for Western blot analysis and stored at −20°C until use.

*Analysis of mitochondrial membrane potential loss*
Changes in MMP following induction of apoptosis were assessed using MitoLight apoptosis detection kit (Chemicon International, Temecula, CA, USA) according to the manufacturer's instructions. In brief, after induction of apoptosis, cells were incubated at 37°C for 15 min in reaction buffer containing MitoLight mitochondrial dye that stained mitochondria in living cells in a membrane potential-dependent fashion. Then, the status of mitochondrial membrane potential was analysed using a FACScan flow cytometer in the FL1 channel.

*RNA isolation and RT–PCR*
Total cellular RNA was isolated using ISOGEN (WAKO, Osaka, Japan). Total RNA (2 $\mu$g) was reverse transcribed using murine Maloney leukemia virus (M-MLV) reverse transcriptase according to the manufacturer's protocols (Promega, Madison, WI, USA). PCR was performed in a total volume of 20 $\mu$l with 1 $\mu$l cDNA synthesis mixture for 25 cycles of 94°C denaturation (1 min), 60°C annealing (1 min), and 72°C extension (1.5 min). PCR primer was as follows. WT1: forward primer, 5′-GACCTGGAATCAGATGAA-3′, reverse primer, 5′-GAGAACTTTCGCTGACAAGTT-3′; Actin: forward primer, 5′-CCCAGCACAATGAAGATCAA GATCAT-3′, reverse primer, 5′-ATCTGCTGGAAGGTGGA CAGCGA-3′.

*Western blot analysis*
Cells were washed twice with PBS and lysed with 2 × Laemmeli's SDS sample buffer. Proteins were separated by SDS–PAGE and transferred to Immobilon polyvinylidene difluoride membrane (Millipore Corp., Bedford, MA, USA). After blocking of non-specific binding, immunoblots were incubated with primary antibody followed by incubation with the appropriate anti-rabbit or anti-mouse IgG antibody conjugated with alkaline phosphatase, and visualized using BCIP/NBT kit (Nacalai Tesque, Kyoto, Japan).

*Activities of caspases*
Caspases 3-like, 9-like, and 8-like activities were measured as described previously (Shimizu *et al.*, 1996). Briefly, the cells were collected at various time points, lysed in lysis buffer (150 mM NaCl, 50 mM Tris-HCl (pH 7.4), 1 mM EDTA, 0.1% Triton-X) on ice for 30 min and centrifuged. The supernatant was stored at −20°C until use. Concentration of proteins was determined using a Bio-Rad protein assay reagent by Bradford method. Then, the cytosol containing 50 $\mu$g of proteins was suspended in reaction buffer (50 mM Tris-HCl (pH 7.4), 1 mM EDTA, and 10 mM EGTA) containing 10 $\mu$M of the enzyme substrate Ac-DEVD-AFC (for caspase-3-like activity), FAM-LEHD-FMK (for caspase-9-like activity), or IETD-pNA (for caspase-8-like activity) and incubated at 37°C for 1 h. The fluorescence at 485/535 nm (for caspases 3- and 9-like activities) or 405 nm (for caspase-8-like activity) was measured using a Spectra-Max Gemini XS fluorescence plate reader (Molecular Devices, Sunnyvale, CA, USA).

*Detection of oligomerization of Bax*
To detect oligomerization of Bax, $2 \times 10^6$ K562 cells were collected, washed three times with PBS, incubated with PBS containing 1 mM of DSS at room temperature for 30 min, and then incubated with 100 mM Tris buffer (pH 7.4) for 15 min to quench the crosslinker.

*Immunocytochemistry*
K562 cells attached onto glass slides by cytocentrifugation were fixed with 4% paraformaldehyde in PBS at room temperature for 20 min. Then, cells were permeabilized with methanol at room temperature for 5 min. After blocking (2% BSA, 0.1% $NaN_3$, 0.2% Tween 20, 6.7% glycerol in PBS) for 45 min, the cells were stained with monoclonal anti-His tag (anti-Xpress) and rabbit anti-mouse IgG conjugated with fluorescein isothiocyanate isomer 1 (FITC) (DAKO, A/S, Denmark). Nucleic acid stain was preformed by using 100 ng/ml DAPI (4′,6-amido-2-phenylindol) (Chemicon, Temecula, CA, USA). For staining of the mitochondria, K562 cells were incubated in the medium containing 100 nM Mitotracker Red 580 (Molecular Probe, Eugene, OR) at 37°C for 30 min. After washes with cell culture medium, cells were observed by laser confocal microscopy, LSM 510 META (Carl Zeiss Inc., Oberkochen, Germany).

*Statistical analysis*
One-way analysis of variance followed by Fisher's PLSD was used to determine the statistical significance of apoptosis employing the STATVIEW software (Abacus Concepts, Inc., Berkeley, CA, USA).

**Acknowledgements**

This work was supported in part by a Grant-in Aid from the Ministry of Education, Science, Sports and Culture and the Ministry of Health, Labour, and Welfare, Japan.

## References

Algar EM, Khromykh T, Smith SI, Blackburn DM, Bryson GJ, Smith PJ. (1996). *Oncogene* **12**: 1005–1014.
Call KM, Glaser TM, Ito CY, Buckler AJ, Pelletier J, Haber DA *et al.* (1990). *Cell* **60**: 509–520.
Davies JA, Ladomery M, Hohenstein P, Michael L, Shafe A, Spraggon L *et al.* (2004). *Hum Mol Genet* **13**: 235–246.
Davies RC, Calvio C, Bratt E, Larsson SH, Lamond AI, Hastie ND. (1998). *Genes Dev* **12**: 3217–3225.
Drummond IA, Madden SL, Rohwer-Nutter P, Bell GI, Sukhatme VP, Rauscher III FJ. (1992). *Science* **257**: 674–678.
Englert C, Maheswaran S, Garvin AJ, Kreidberg J, Haber DA. (1997). *Cancer Res* **8**: 1429–1434.
Gashler AL, Bonthouron DT, Madden SL, Rauscher III FJ, Collins T, Sukhatme VP. (1992). *Proc Natl Acad Sci USA* **89**: 10984–10988.
Goodyer P, Dehbi M, Torban E, Bruening W, Pelletier J. (1995). *Oncogene* **10**: 1125–1129.
Harada Y, Nonomura N, Nishimura K, Tamaki H, Takahara S, Miki T *et al.* (1999). *Mol Urol* **3**: 357–364.
Harrington MA, Konicek B, Song A, Xia XL, Fredericks WJ, Rauscher III FJ. (1993). *J Biol Chem* **268**: 21271–21275.
Herzer U, Crocoll A, Barton D, Howells N, Englert C. (1999). *Curr Biol* **9**: 837–840.
Hubinger G, Schmid M, Linortner S, Manegold A, Bergmann L, Maurer U. (2001). *Exp Hematol* **10**: 1226–1235.
Inoue K, Sugiyama H, Ogawa H, Nakagawa M, Yamagami T, Miwa H *et al.* (1994). *Blood* **84**: 3071–3079.
Inoue K, Tamaki H, Ogawa H, Oka Y, Soma T, Tatekawa T *et al.* (1998). *Blood* **91**: 2969–2976.
Kreidberg JA, Sariola H, Loring JM, Maeda M, Pelletier J, Housman D *et al.* (1993). *Cell* **74**: 679–691.
Larsson SH, Charlieu JP, Miyagawa K, Engelkamp D, Rassoulzadegan M, Ross A *et al.* (1995). *Cell* **81**: 391–401.
Li H, Oka Y, Tsuboi A, Yamagami T, Miyazaki T, Yusa S *et al.* (2003). *Int J Hematol* **77**: 463–470.
Loeb DM, Evron E, Patel CB, Sharma PM, Niranjan B, Buluwela L *et al.* (2001). *Cancer Res* **61**: 921–925.
Loeb DM, Summers JL, Burwell EA, Korz D, Friedman AD, Sukumar S. (2003). *Leukemia* **17**: 965–971.
Mayo MW, Wang CY, Drouin SS, Madrid LV, Marshall AF, Reed JC *et al.* (1999). *EMBO J* **18**: 3990–4003.
Miyoshi Y, Ando A, Egawa C, Taguchi T, Tamaki Y, Tamaki H *et al.* (2002). *Clin Cancer Res* **8**: 1167–1171.
Niksic M, Slight J, Sanford JR, Caceres JF, Hastie ND. (2004). *Hum Mol Genet* **13**: 463–471.
Oji Y, Inohara H, Nakazawa M, Nakano Y, Akahani S, Nakatsuka S *et al.* (2003a). *Cancer Sci* **94**: 523–529.
Oji Y, Miyoshi S, Maeda H, Hayashi S, Tamaki H, Nakatsuka S *et al.* (2002). *Int J Cancer* **100**: 297–303.
Oji Y, Miyoshi Y, Koga S, Nakano Y, Ando A, Nakatsuka S *et al.* (2003b). *Cancer Sci* **94**: 606–611.
Oji Y, Nakamori S, Fujikawa M, Nakatsuka S, Yokota A, Tatsumi N *et al.* (2004a). *Cancer Sci* **95**: 583–587.
Oji Y, Ogawa H, Tamaki H, Oka Y, Tsuboi A, Kim EH *et al.* (1999). *Jpn J Cancer Res* **90**: 194–204.
Oji Y, Suzuki T, Nakano Y, Maruno M, Nakatsuka S, Jomgeow T *et al.* (2004b). *Cancer Sci* **95**: 822–827.
Oji Y, Yamamoto H, Nomura M, Nakano Y, Ikeba A, Nakatsuka S *et al.* (2003c). *Cancer Sci* **94**: 712–717.
Oji Y, Yano M, Nakano Y, Abeno S, Nakatsuka S, Ikeba A *et al.* (2004c). *Anticancer Res* **24**: 3103–3108.
Osaka M, Koami K, Sugiyama T. (1997). *Int J Cancer* **72**: 696–699.
Reynolds PA, Smolen GA, Palmer RE, Sgroi D, Yajnik V, Gerald WL *et al.* (2003). *Genes Dev* **17**: 2094–2107.
Shimizu S, Eguchi Y, Kamiike W, Matsuda H, Tsujimoto Y. (1996). *Oncogene* **12**: 2251–2257.
Siehl JM, Reinwald M, Heufelder K, Menssen HD, Keilholz U, Thiel E. (2000). *Ann Hematol* **83**: 745–750.
Sugiyama H. (2001). *Int J Hematol* **73**: 177–187.
Tsuboi A, Oka Y, Ogawa H, Elisseeva OA, Tamaki H, Oji Y *et al.* (1999). *Leuk Res* **23**: 499–505.
Tuna M, Chavez-Reyes A, Tari AM. (2005). *Oncogene* **24**: 1648–1652.
Ueda T, Oji Y, Naka N, Nakano Y, Takahashi E, Koga S *et al.* (2003). *Cancer Sci* **3**: 271–276.
Wagner KD, Wagner N, Vidal VP, Schley G, Wilhelm D, Schedl A *et al.* (2002). *EMBO J* **21**: 1398–1405.
Werner H, Re GG, Drummond IA, Sukhatme VP, Rauscher III FJ, Sens DA *et al.* (1993). *Proc Natl Acad Sci USA* **90**: 5828–5832.
Yamagami T, Ogawa H, Tamaki H, Oji Y, Soma T, Oka Y *et al.* (1998). *Leuk Res* **22**: 383–384.
Yamagami T, Sugiyama H, Inuoe K, Ogawa H, Tatekawa T, Hirata M *et al.* (1996). *Blood* **87**: 2878–2884.

Apoptosis
DOI 10.1007/s10495-006-0525-7

# Role of the mitochondrial membrane permeability transition in cell death

Yoshihide Tsujimoto · Shigeomi Shimizu

Published online: 21 November 2006


**Abstract** In recent years, the role of the mitochondria in both apoptotic and necrotic cell death has received considerable attention. An increase of mitochondrial membrane permeability is one of the key events in apoptotic or necrotic death, although the details of the mechanism involved remain to be elucidated. The mitochondrial membrane permeability transition (MPT) is a $Ca^{2+}$-dependent increase of mitochondrial membrane permeability that leads to loss of $\Delta\psi$, mitochondrial swelling, and rupture of the outer mitochondrial membrane. The MPT is thought to occur after the opening of a channel that is known as the permeability transition pore (PTP), which putatively consists of the voltage-dependent anion channel (VDAC), the adenine nucleotide translocator (ANT), cyclophilin D (Cyp D: a mitochondrial peptidyl prolyl-*cis*, *trans*-isomerase), and other molecule(s). Recently, significant progress has been made by studies performed with mice lacking Cyp D at several laboratories, which have convincingly demonstrated that Cyp D is essential for the MPT to occur and that the Cyp D-dependent MPT regulates some forms of necrotic, but not apoptotic, cell death. Cyp D-deficient mice have also been used to show that the Cyp D-dependent MPT plays a crucial role in ischemia/reperfusion injury. The anti-apoptotic proteins Bcl-2 and Bcl-$x_L$ have the ability to block the MPT, and can therefore block MPT-dependent necrosis in addition to their well-established ability to inhibit apoptosis.

Y. Tsujimoto (✉) · S. Shimizu
Osaka University Medical School, Department of Medical Genetics, SORST of the Japan Science and Technology Agency, 2-2 Yamadaoka, Suita, Osaka 565-0871, Japan

**Keywords** Apoptosis · Necrosis · Mitochondria · Cyclophilin D · Cyclosporin A · Membrane permeability transition · Cytochrome c · Ischemia

## Introduction

Apoptosis is a form of programmed cell death and an outline of the relevant signaling pathways at the molecular level is now well established. Mammalian cells possess two major apoptotic signaling pathways, which are known as the intrinsic pathway and the extrinsic pathway [1]. The intrinsic pathway involves an increase of outer mitochondrial membrane permeability that leads to the release of various proteins from the intermembrane space into the cytoplasm, including apoptogenic molecules such as cytochrome *c*, Smac/Diablo, HtrA2 (Omi), AIF, and DNaseG [1, 2]. In the presence of ATP (dATP), cytochrome *c* binds to Apaf-1 and triggers its oligomerization, after which pro-caspase-9 is recruited and undergoes autoactivation. The protein complex comprising cytochrome *c*, Apaf-1, and caspase-9 is called the "apoptosome". In short, an increase of outer mitochondrial membrane permeability is central to apoptosis [3, 4], and mitochondrial membrane permeability is directly regulated by the Bcl-2 family of proteins [4, 5] (see Fig. 1). However, the detailed mechanisms underlying the increase of outer mitochondrial membrane permeability during apoptosis and how this process is controlled by Bc1-2 family members are still to be determined. The model that was initially developed to explain the apoptotic increase of mitochondrial membrane permeability was based on the "mitochondrial membrane permeability transition" (MPT) [6], an event which has been appreciated for some time among investigators studying the mitochondria. This review summarizes recent progress with

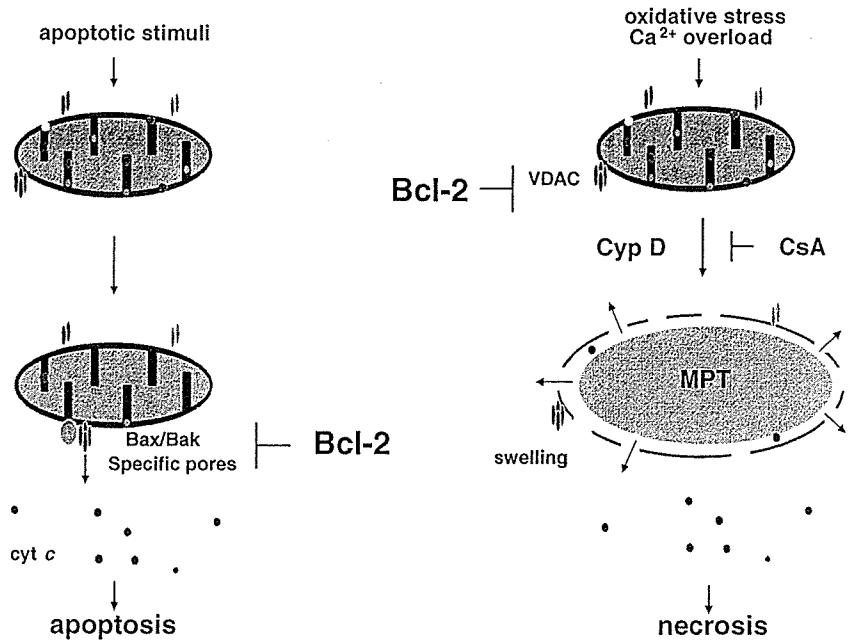


Fig. 1 Role of the mitochondria in apoptosis and necrosis. An increase in the permeability of the outer mitochondrial membrane is crucial for apoptosis to occur and is regulated by multidomain pro-apoptotic members of the Bcl-2 family (Bax and Bak), resulting in the release of several apoptogenic factors into the cytoplasm. In contrast, the Cyp D-dependent MPT involves an increase in the permeability of both the outer and inner mitochondrial membranes, and leads to necrosis induced by $Ca^{2+}$ overload and oxidative stress. Both types of mitochondrial membrane permeability change are inhibited by anti-apoptotic members of the Bcl-2 family (Bcl-2 and Bcl-$x_L$)

regard to our understanding of the role of the MPT in cell death.

## MPT

Mitochondria isolated from a variety of sources can show a sudden increase in the permeability of the inner mitochondrial membrane to solutes with a molecular mass of less than 1,500 Da, which results in the loss of $\Delta\psi$, mitochondrial swelling, and rupture of the outer mitochondrial membrane [7, 8] (see Fig. 1). This process is called the mitochondrial membrane permeability transition (MPT). The MPT can be induced under various conditions, such as exposure of mitochondria to $Ca^{2+}$ together with inorganic phosphate. Although the molecular mechanisms of the MPT are largely unknown, the most widely accepted model (working hypothesis) is that it occurs after the opening of a channel complex that has been termed the permeability transition pore (PTP), which is thought to consist of the voltage-dependent anion channel (VDAC: outer membrane channel), the adenine nucleotide translocator (ANT: inner membrane channel), cyclophilin D (Cyp D), and possibly other molecule(s) [9] (see Fig. 2). However, it still remains uncertain whether the PTP really exists and what its exact nature is. Moreover, several experimental findings are difficult to explain by this model (see the introduction of [10]). A role of the ANT in the MPT is supported by MPT inhibition and activation by bonkrekic acid and atractyloside, respectively, which are ANT ligands [11]. Cyp D is a mitochondrial member of the cyclophilin family, which possesses peptidyl prolyl-*cis*, *trans*-isomerase (PPIase) activity and has a crucial role in protein folding [12]. The putative role of Cyp D in regulating the MPT is based on the observation that cyclosporin A (CsA), a specific inhibitor of the cyclophilin family, blocks the MPT [13]. Since CsA inhibits PPIase and the MPT at similar concentrations, PPIase activity may be critical for the MPT to occur. Cyp D resides in the mitochondrial matrix, but becomes associated with the inner mitochondrial membrane during the MPT. Based on the enzymatic activity of Cyp D as a PPIase, it may induce a conformational change of an inner membrane channel such as the ANT that leads to an increase of inner membrane permeability. In addition to the CsA-sensitive and $Ca^{2+}$-dependent ("regulated") MPT, the existence of a CsA-insensitive ("unregulated") MPT has also been suggested, although its mechanism and relationship to the CsA-sensitive MPT are totally unknown [10].

In the mid-1990s, the MPT attracted the attention of investigators in the cell death field, because it was reported that at least some forms of apoptosis could be inhibited by CsA, suggesting a role of the CsA-sensitive MPT in this process of cell death [9, 14]. A possible role of the MPT in apoptosis is also supported by the finding that apoptosis can sometimes be inhibited by bonkrekic acid [11, 15]. The CsA-sensitive MPT has also been implicated in remodeling of the mitochondrial cristae and mobilization of cytochrome *c* stores from the cristae during apoptosis, which promotes the complete release of cytochrome *c* [16]. However, the overall role of the MPT in apoptosis was still controversial, because there have been a number of reports that apoptosis

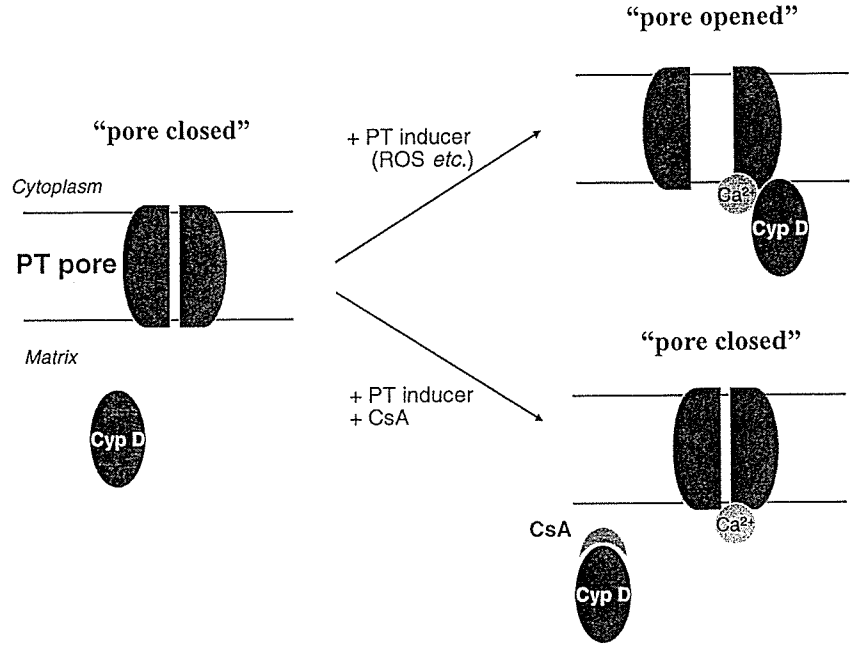


**Fig. 2** Model of the MPT pore Under normal conditions, Cyp D is localized to the mitochondrial matrix, and the MPT pore is closed. In the presence of permeability transition inducers, Cyp D is considered to bind to and induce a conformational change of a channel in the inner membrane, resulting in opening of the MPT pore. Cyclosporin A (CsA) binds to and inhibits Cyp D to prevent MPT pore opening

is not inhibited by CsA [17]. Also, it has been demonstrated that $\Delta\psi$ occurs after cytochrome *c* release in at least some types of apoptosis, suggesting that the MPT is not always the trigger for cytochrome *c* release and cell death. This issue was recently been solved by studies performed in Cyp D-deficient mice, as discussed later.

## Are the VDAC, the ANT, and Cyp D essential for the MPT?

It has long been thought that the VDAC, the ANT, and Cyp D play an essential role in the MPT, but convincing evidence was lacking until very recently.

An important role of the VDAC in the MPT has been supported by the following findings: (1) the electrophysiological properties of the PTP are strikingly similar to those of the VDAC incorporated in planar phospholipids bilayers [18, 19]; (2) various factors that alter VDAC channel properties, such as addition of NADH, $Ca^{2+}$, or glutamate, as well as binding to hexokinase II [20–24], also modulate PTP activity [25–27]; and (3) chromatography of mitochondrial extracts on a Cyp D affinity column leads to purification of the VDAC associated with the ANT [28].

The most convincing evidence about involvement of the VDAC in the MPT should theoretically be obtained by studies employing VDAC-deficient cells. Such a study was recently performed with mitochondria isolated from VDAC1-deficient cells, and it was found that VDAC1-deficient mitochondria still undergo the MPT normally, suggesting that VDAC1 is not important for this process. However, this result could have been due to compensation for VDAC1 deficiency by other isoforms, including VDAC2 and VDAC3. So far, experimental evidence for a direct role of the VDAC in the MPT has been provided by studies using specific anti-VDAC antibodies [29]. Two polyclonal anti-VDAC antibodies, which recognize different VDAC epitopes and inhibit its activity in liposomes [29], have been shown to inhibit the $Ca^{2+}$-induced MPT [29], supporting a crucial role for the VDAC in this process.

The ANTs (ANT1 and 2 in mice and ANT1, 2, and 3 in humans) are also considered to be important for the MPT. It has been demonstrated that Cyp D interacts directly with the ANT, although it is not known whether CsA inhibits this interaction [28, 30]. Regarding the role of the ANT in the MPT, considerable progress was made recently because it was shown that liver mitochondria from mice lacking both ANT1 and ANT2 still underwent the MPT, although the triggering $Ca^{2+}$ concentration was slightly increased [31]. This finding suggests that ANT1/2 only play a limited role, if any, in the MPT or else that deficiency of ANT1/2 was compensated by other channel(s). The lack of an important role for the ANT in the MPT would be consistent with the observation that mitochondria isolated from yeast lacking the ANT still undergo MPT-like changes, including loss of membrane potential and swelling in response to ethanol, which are very similar events to those occurring in mammalian mitochondria during the MPT [32]. However, it is unknown whether

yeast mitochondria undergo a real MPT, because swelling of these mitochondria and loss of membrane potential in response to ethanol are not inhibited by CsA, although this inability of CsA to inhibit MPT-like events might be due to its inability to inhibit a Cyp D counterpart in yeast mitochondria. If the ANT is not involved in the MPT, the other channel(s) that are actually involved might be ANT-like inner membrane channels, because the MPT is modulated by ANT ligands such as bonkrekic acid or atractyloside and is accompanied by loss of $\Delta\psi$ (i.e., increased permeability of the inner mitochondrial membrane). Identification of one or more channels in the inner mitochondrial membrane that are directly involved in the MPT and might be targets of Cyp D would be an important step forward.

The role of Cyp D in the MPT was initially suggested by the finding that the MPT is blocked by CsA, which is known to inhibit the PPIase activity of cyclophilins. This finding has recently been confirmed by studies performed employing Cyp D gene (*ppif*)-deficient mice [33–36]. It has been demonstrated that Cyp D-deficient mitochondria isolated from the livers of these mice do not undergo the CsA-sensitive MPT in response to a variety of inducers, including $Ca^{2+}$, atractyloside, and $H_2O_2$. Because the MPT does not occur, these mitochondria accumulate a much higher concentration of $Ca^{2+}$ than control mitochondria [33, 36]. However, the CsA-insensitive MPT (with loss of $\Delta\psi$ and swelling) can still occur when these Cyp D-deficient mitochondria are exposed to high concentrations of $Ca^{2+}$ [33, 35]. In addition, Cyp D-deficient mitochondria show a normal response to reagents like ubiquinone and thiol oxidants that cause the CsA-insensitive MPT [35]. The CsA-sensitive MPT and CsA-insensitive MPT might share a common mechanism, because both forms of MPT are inhibited by ubiquinone 0 [35]. This finding might also suggest that Cyp D only sensitizes the mitochondria to the $Ca^{2+}$-induced MPT, although these two forms of MPT might be mediated by different mechanisms. This issue will only be solved by identification of the essential players involved in the MPT. In any case, it has been confirmed that Cyp D has a specific role in the CsA-sensitive MPT.

Although it is now clear that the Cyp D is an essential component of the CsA-sensitive MPT, there are still many questions to be answered. More studies are needed to elucidate the molecular nature of the MPT pore complex. Assuming that Cyp D interacts as a PPIase with other molecules essential for the MPT that probably reside in the inner mitochondrial membrane, a promising approach would be the isolation of a protein complex containing Cyp D and the VDAC. Another issue would be investigation of the relationship between the Cyp D-dependent MPT and the unregulated MPT. Furthermore, does the unregulated MPT have a role in apoptosis or other forms of cell death?

## Role of the MPT

For a long time, it has been unclear whether the CsA-sensitive MPT plays an important role in the apoptotic increase of mitochondrial membrane permeability. However, studies of Cyp D-deficient mice have finally solved this issue. Various cells isolated from Cyp D-deficient mice, such as thymocytes, embryonic fibroblasts (MEFs), and hepatocytes, undergo apoptosis normally in response to various stimuli, including etoposide, stautosporine, and tumor necrosis factor-$\alpha$ [33–36]. Small intestinal cells from Cyp D-deficient mice are also as sensitive to X ray-induced apoptosis as cells from control mice [33]. These results provide the most compelling evidence that the CsA-sensitive MPT is not essential for apoptosis. Of course, it remains possible that some forms of apoptosis might be mediated by the CsA-sensitive MPT, and thus inhibited by CsA. However, the inhibitory effect of CsA on apoptosis might need to be more carefully evaluated because it is usually studied at relatively high CsA concentrations that could inhibit other targets, including cytoplasmic cyclophilins involved in transcriptional regulation, thus having a secondary effect on apoptosis. Accordingly, it may be necessary to re-evaluate CsA-dependent inhibition of apoptosis by using Cyp D-deficient cells or by silencing Cyp D to assess the real effect of CsA.

Several studies have indicated that overexpression of Cyp D protects cells against some forms of apoptosis. For example, the overexpression of CypD inhibits apoptosis induced by overexpression of caspase-8 (but not Bax) or by exposure to arsenic trioxide [37, 38]. It may be possible that these forms of apoptosis are mediated by the MPT, which is somehow affected by Cyp D overexpression. However, studies of transgenic mice with myocardial expression of Cyp D have revealed that cardiac myocytes isolated from these mice show a tendency to undergo mitochondrial swelling and spontaneous death [34], suggesting that the effects of Cyp D expression might be cell type-specific.

In contrast to the lack of any influence of Cyp D deficiency on apoptosis, the Cyp D-dependent MPT plays an important role in some forms of necrotic cell death (see Fig. 1). Cyp D-deficient MEFs show significantly increased resistance to $H_2O_2$-induced necrosis [33, 34], and Cyp D-deficient hepatocytes display resistance to necrosis induced by a $Ca^{2+}$ ionophore (A23187) or by $H_2O_2$ [33, 34]. Interestingly, when $H_2O_2$-induced and $Ca^{2+}$ ionophore-induced necrosis is inhibited by Cyp D deficiency in these cells, apoptosis does not occur as an alternate death mechanism [33], suggesting that the $H_2O_2/Ca^{2+}$-triggered apoptotic signaling pathways are somehow blocked in these types of cells.

Another very interesting question concerns the biological significance of the MPT because it is conceivable that the MPT plays a role in some physiological processes. By

analyzing Cyp D-deficient mice and cells in more detail, some hints about the role of the MPT should be obtained.

## Regulation of the MPT by Bcl-2

Anti-apoptotic members of the Bcl-2 family, such as Bcl-2 itself and Bcl-$x_L$, are known to inhibit the Bax/Bak-dependent apoptotic increase of mitochondrial membrane permeability by direct interaction with pro-apoptotic members of this family, and also inhibit the MPT itself [39, 40] (see Fig. 1). How do these proteins block the MPT? Given that Bax/Bak is not essential for the MPT [33], Bcl-2 (Bcl-$x_L$) might directly inhibit a component of the PTP complex. In fact, Bcl-2 (Bcl-$x_L$) is capable of blocking VDAC activity [39] and ANT activity in liposome systems [41]. As described above, the VDAC plays a role in the MPT [29], whereas the ANT might not be important [31], so Bcl-2 and Bcl-$x_L$ possibly inhibit the MPT by blocking the VDAC or unknown channels similar to the ANT that are actually involved in the MPT.

## Role of the Cyp D-dependent MPT in disease

The advent of Cyp D-deficient mice has provided compelling evidence that the Cyp D-dependent MPT plays a crucial role in ischemia/reperfusion injury affecting the heart [33, 34] and brain [36], suggesting that the Cyp D-dependent MPT is involved in ischemia/reperfusion-induced cell death and that Cyp D and other components of the MPT are promising therapeutic targets. However, there have been a large number of reports published on the death mechanisms of ischemia/reperfusion injury and investigation of therapeutic methods, making it evident that ischemia/reperfusion injury is a very complex phenomenon which might involve multiple death mechanisms, because such injury can be suppressed by various inhibitors of different forms of cell death. It has been shown that ischemia/reperfusion injury can be ameliorated by inhibiting apoptosis with caspase inhibitors [42–45], inhibiting necroptosis with Nec1 [46], or blocking the Ask 1 pathway [47]. In studies of model systems employing cell lines, the death mechanisms involving caspases, a Nec1 target, Ask1, and the Cyp D-dependent MPT do not seem to overlap with each other. Why are so many different potential mechanisms involved in ischemia/reperfusion injury? Different death mechanisms might operate in the same cell in a sequential manner or in parallel, meaning that the inhibition of one mechanism might have a protective effect. Alternatively, different death mechanisms might act on different cells during ischemia/reperfusion injury and the dying cells might trigger the death process in other cells. It is also possible that different cell death mechanisms are activated by different ischemic conditions. For further studies of ischemia/reperfusion injury, mice that lack certain cell death mechanisms, such as Cyp D-deficient mice and Bax/Bak-deficient mice, would be useful tools.

The Cyp D-dependent MPT might also be involved in other diseases. It has been reported that mitochondria isolated from the livers of MND2 mice with mutation of the omi gene are more susceptible to the MPT [48]. MND2 mice succumb to motoneuron disease [49], which might be caused by the MPT occurring at a lower threshold in neuronal mitochondria. Thus, future studies may unveil a role of the Cyp D-dependent MPT in the pathogenesis of various diseases.

**Acknowledgments** The studies performed at our laboratory were partly supported by a grant for the 21st century COE Program, a grant for Scientific Research from the Ministry of Education, Science, Sports, and Culture of Japan, and a grant for Research on Dementia and Fracture from the Ministry of Health, Labour and Welfare of Japan.

## References

1. Green DR, Evan GI (2002) A matter of life and death. Cancer Cell 1:19–30
2. Wang X (2001) The expanding role of mitochondria in apoptosis. Genes Dev 15:2922–2933
3. Desagher S, Martinou JC (2000) Mitochondria as the central control point of apoptosis. Trends Cell Biol 10:369–377
4. Tsujimoto Y (2003) Cell death regulation by the Bcl-2 protein family in the mitochondria. J Cell Physiol 195:158–167
5. Adams JM, Cory S (2001) Life-or-death decisions by the Bcl-2 protein family. Trends Biochem Sci 26:61–66
6. Kroemer G, Petit P, Zamzami N, Vayssiere JL, Mignotte B (1995) The biochemistry of programmed cell death. FASEB J 9:1277–1287
7. Zoratti M, Szabo I (1995) The mitochondrial permeability transition. Biochim Biophys Acta 1241:139–176
8. Halestrap AP, McStay GP, Clarke SJ (2002) The permeability transition pore complex: another view. Biochimie 84:153–166
9. Crompton M (2003) On the involvement of mitochondrial intermembrane junctional complexes in apoptosis. Curr Med Chem 10:1473–1484
10. He L, Lemasters JJ (2002) Regulated and unregulated mitochondrial permeability transition pores: a new paradigm of pore structure and function? FEBS Lett 512:1–7
11. Zamzami N, Kroemer G (2001) The michondrion in apoptosis: how Pandora's box opens. Nature Rev Mol Cell Biol 2:67–71
12. Galat A, Metcalfe SM (1995) Peptidylproline cis/trans isomerases. Prog Biophys Mol Biol 63:67–118
13. Broekemeier KM, Dempsey ME, Pfeiffer DR (1989) Cyclosporin A is a potent inhibitor of the inner membrane permeability transition in liver mitochondria. J Biol Chem 264:7826–7830
14. Green DR, Kroemer G (2004) The pathophysiology of mitochondrial cell death. Science 305:626–629
15. Zamzami N, Susin SA, Marchetti P, Hirsch T, Gomez-Monterrey I, Castedo M, Kroemer G (1996) Mitochondrial control of nuclear apoptosis. J Exp Med 183:1533–1544
16. Scorrano L, Ashiya M, Buttle K, Weiler S, Oakes SA, Mannella CA, Korsmeyer SJ (2002) A distinct pathway remodels mitochondrial cristae and mobilizes cytochrome *c* during apoptosis. Dev Cell 2:55–67

17. Newmeyer DD, Ferguson-Miller S (2003) Mitochondria: releasing power for life and unleashing the machineries of death. Cell 112:481–490
18. Szabo I, Zoratti M (1993) The mitochondrial permeability transition pore may comprise VDAC molecules. I. Binary structure and voltage dependence of the pore. FEBS Lett 330:201–205
19. Szabo I, De Pinto V, Zoratti M (1993) The mitochondrial permeability transition pore may comprise VDAC molecules. II. The electrophysiological properties of VDAC are compatible with those of the mitochondrial megachannel. FEBS Lett 330:206–210
20. Zizi M, Forte M, Blachly-Dyson E, Colombini M (1994) NADH regulates the gating of VDAC, the mitochondrial outer membrane channel. J Biol Chem 269:1614–1616
21. Gincel D, Zaid H, Shoshan-Barmatz V (2001) Calcium binding and translocation by the voltage-dependent anion channel: a possible regulatory mechanism in mitochondrial function. Biochem J 358(Pt 1):147–155
22. Gincel D, Shoshan-Barmatz V (2004) Glutamate interacts with VDAC and modulates opening of the mitochondrial permeability transition pore. J Bioenerg Biomembr 36:179–186
23. Pastorino JG, Shulga N, Hoek JB (2002) Mitochondrial binding of hexokinase II inhibits Bax-induced cytochrome *c* release and apoptosis. J Biol Chem 277:7610–7618
24. Pastorino JG, Hoek JB, Shulga N (2005) Activation of glycogen synthase kinase 3beta disrupts the binding of hexokinase II to mitochondria by phosphorylating voltage-dependent anion channel and potentiates chemotherapy-induced cytotoxicity. Cancer Res 65:10545–10554
25. Costantini P, Chernyak BV, Petronilli V, Bernardi P (1996) Modulation of the mitochondrial permeability transition pore by pyridine nucleotides and dithiol oxidation at two separate sites. J Biol Chem 271:6746–6751
26. Fontaine E, Eriksson O, Ichas F, Bernardi P (1998) Regulation of the permeability transition pore in skeletal muscle mitochondria. Modulation By electron flow through the respiratory chain complex i. J Biol Chem 1998 273:12662–12668
27. Pastorino JG, Hoek JB (2003) Hexokinase II: the integration of energy metabolism and control of apoptosis. Curr Med Chem 10:1535–1551
28. Crompton M, Virji S, Ward JM (1998) Cyclophilin-D binds strongly to complexes of the voltage-dependent anion channel and the adenine nucleotide translocase to form the permeability transition pore. Eur J Biochem 258:729–735
29. Shimizu S, Matsuoka Y, Shinohara Y, Yoneda Y, Tsujimoto Y (2001) Essential role of voltage-dependent anion channel in various forms of apoptosis in mammalian cells. J Cell Biol 152:237–250
30. Woodfield K, Ruck A, Brdiczka D, Halestrap AP (1998) Direct demonstration of a specific interaction between cyclophilin-D and the adenine nucleotide translocase confirms their role in the mitochondrial permeability transition. Biochem J 336:287–290
31. Kokoszka JE, Waymire KG, Levy SE, Sligh JE, Cai J, Jones DP, MacGregor GR, Wallace DC (2004) The ADP/ATP translocator is not essential for the mitochondrial permeability transition pore. Nature 427:461–465.
32. Shimizu S, Shinohara Y, Tsujimoto Y (2000) Bax and Bcl-xL independently regulate apoptotic changes of yeast mitochondria that require VDAC but not adenine nucleotide translocator. Oncogene 19:4309–4318
33. Nakagawa T, Shimizu S, Watanabe T, Yamaguchi O, Otsu K, Yamagata H, Inohara H, Kubo T, Tsujimoto Y (2005) Cyclophilin D-dependent mitochondrial permeability transition regulates some necrotic but not apoptotic death. Nature 434:652–658
34. Baines CP, Kaiser RA, Purcell NH, Blair NS, Osinska H, Hambleton MA, Brunskill EW, Sayen MR, Gottlieb RA, Dorn GW, Robbins J, Molkentin JD (2005) Loss of cyclophilin D reveals a critical role for mitochondrial permeability transition in cell death. Nature 434:658–662
35. Basso E, Fante L, Fowlkes J, Petronilli V, Forte MA, Bernardi P (2005) Properties of the permeability transition pore in mitochondria devoid of cyclophilin D. J Biol Chem 280:18558–18561
36. Schinzel AC, Takeuchi O, Huang Z, Fisher JK, Zhou Z, Rubens J, Hetz C, Danial NN, Moskowitz MA, Korsmeyer SJ (2005) Cyclophilin D is a component of mitochondrial permeability transition and mediates neuronal cell death after focal cerebral ischemia. Proc Natl Acad Sci USA 102:12005–12010
37. Lin DT, Lechleiter JD (2002) Mitochondrial targeted cyclophilin D protects cells from cell death by peptidyl prolyl isomerization. J Biol Chem 277:31134–31141
38. Schubert A, Grimm S (2004) Cyclophilin D, a component of the permeability transition pore, is an apoptosis repressor. Cancer Res 64:85–93
39. Shimizu S, Eguchi Y, Kamiike W, Funahashi Y, Mignon A, Lacronique V, Matsuda H, Tsujimoto Y (1998) Bcl-2 prevents apoptotic mitochondrial dysfunction by regulating proton flux. Proc Natl Acad Sci USA 95:1455–1459
40. Reed JC, Kroemer G (1998) The permeability transition pore complex: a target for apoptosis regulation by caspases and Bcl-2-related proteins. J Exp Med 187:1261–1271
41. Marzo I, Brenner C, Zamzami N, Jurgensmeier JM, Susin SA, Vieira HL, Prevost MC, Xie Z, Matsuyama S, Reed JC, Kroemer G (1998) Bax and adenine nucleotide translocator cooperate in the mitochondrial control of apoptosis. Science 281:2027–2031
42. Cheng Y, Deshmukh M, D'Costa A, Demaro JA, Gidday JM, Shah A, Sun Y, Jacquin MF, Johnson EM, Holtzman DM (1998) Caspase inhibitor affords neuroprotection with delayed administration in a rat model of neonatal hypoxic-ischemic brain injury. J Clin Invest 101:1992–1999
43. Chen J, Nagayama T, Jin K, Stetler RA, Zhu RL, Graham SH, Simon RP (1998) Induction of caspase-3-like protease may mediate delayed neuronal death in the hippocampus after transient cerebral ischemia. J Neurosci 18:4914–4928
44. Xu D, Bureau Y, McIntyre DC, Nicholson DW, Liston P, Zhu Y, Fong WG, Crocker SJ, Korneluk RG, Robertson GS (1999) Attenuation of ischemia-induced cellular and behavioral deficits by X chromosome-linked inhibitor of apoptosis protein overexpression in the rat hippocampus. J Neurosci 19:5026–5033
45. Bott-Flugel L, Weig HJ, Knodler M, Stadele C, Moretti A, Laugwitz KL, Seyfarth M (2005) Gene transfer of the pancaspase inhibitor P35 reduces myocardial infarct size and improves cardiac function. J Mol Med 83:526–534
46. Degterev A, Huang Z, Boyce M, Li Y, Jagtap P, Mizushima N, Cuny GD, Mitchison TJ, Moskowitz MA, Yuan J (2005) Chemical inhibitor of nonapoptotic cell death with therapeutic potential for ischemic brain injury. Nat Chem Biol 1:112–119
47. Watanabe T, Otsu K, Takeda T, Yamaguchi O, Hikoso S, Kashiwase K, Higuchi Y, Taniike M, Nakai A, Matsumura Y, Nishida K, Ichijo H, Hori M (2005) Apoptosis signal-regulating kinase 1 is involved not only in apoptosis but also in non-apoptotic cardiomyocyte death. Biochem Biophys Res Commun 333:562–527
48. Jones JM, Datta P, Srinivasula SM, Ji W, Gupta S, Zhang Z, Davies E, Hajnoczky G, Saunders TL, Van Keuren ML, Fernandes-Alnemri T, Meisler MH, Alnemri ES (2003) Loss of Omi mitochondrial protease activity causes the neuromuscular disorder of mnd2 mutant mice. Nature 425:721–727
49. Jones JM, Albin RL, Feldman EL, Simin K, Schuster TG, Dunnick WA, Collins JT, Chrisp CE, Taylor BA, Meisler MH (1993) mnd2: a new mouse model of inherited motor neuron disease. Genomics 16:669–677

J Med Primatol doi:10.1111/j.1600-0684.2006.00187.x

CASE HISTORY

# Quantitation of sleep and spinal curvature in an unusually longevous owl monkey (*Aotus azarae*)

Juri Suzuki & Sachi Sri Kantha

Center for Human Evolution Modeling Research, Kyoto University-Primate Research Institute, Inuyama City, Japan

**Keywords**
aging – captive – Cebidae – kyphosis – longevity – nocturnality – radiography

**Correspondence**
Juri Suzuki, Center for Human Evolution Modeling Research, Primate Research Institute, Kyoto University, Inuyama 484 8506, Japan.
Tel.: +81 568 63 0586;
fax: +81 568 62 9559;
e-mail: suzuki@pri.kyoto-u.ac.jp

Accepted May 31, 2006.

## Abstract

*Background* A table summarizing the primary literature on 19 species of longevous non-human primates, other than owl monkey, is presented.
*Methods* We prospectively quantitated the sleep of a longevous female owl monkey (*Aotus azarae*), aged >30 years, longitudinally for 2 years and also evaluated the senility-induced change in spinal curvature.
*Results* The mean daily total sleep time (TST) of this monkey ranged between 790 and 1106 minutes, and was markedly higher in comparison with its female progeny (aged 16 years and used as a control) whose daily TST during the same experimental period ranged between 612 and 822 minutes.
*Conclusion* The calculated kyphotic index (KI) of 2.27 for this monkey, compared with the KIs 4.83 and 5.42, for its progeny and female grandprogeny (aged 1 year) respectively, confirmed the prominent spinal curvature.

## Introduction

Although the longevity quantitation of non-human primates living in the wild is susceptible to higher degree of doubt and imprecision, in the past five decades more reliable quantitation of longevity among captive non-human primates have become feasible. Based on previously published longevity reports on captive primates [6, 27, 41], longevous status among the four major non-human primate groups can be arbitrarily fixed as, >40 years for apes, >30 years for Old World monkeys, >20 years for New World monkeys and >10 years for Prosimians. Table 1 provides a select list of original reports which have appeared since 1969 on 19 species of longevous non-human primates held in captivity. As one could expect, majority of these reports were retrospective studies representing clinicopathological investigations based on the postmortem specimens of tissues and bones. Prospective studies on longevous non-human primates have been sparse at best. In addition, reports on the longevous owl monkey (*Aotus*) have been lacking.

Among the more than 230 species of non-human primates, the owl monkey is unique in being the only nocturnally adapted Anthropoidean primate [4, 39, 44]. Owl monkeys are strictly arboreal and lead a monogamous family life, with a group size of two to five members consisting of a breeding pair and young progeny. Young members emigrate from the family group when they complete the subadult stage by the end of 3 years [59]. The life span of owl monkey in the wild remains yet to be clarified [16], though 12–20 years [22] and 26–30 years [16] have been noted as plausible longevity ranges for owl monkeys under captive conditions.

As of now, the only available report on aged owl monkeys [13] relates to histopathological examination of postmortem brain tissues, as a primate representative, on a comparative scan on the neuropathology of aging in the brains of 47 vertebrate species. Unfortunately, the ages of the two owl monkeys studied for the presence of lipofuscin pigment, argyrophilic plaques, neurofibrillary tangles and corpora amylacea have not been stated.

The owl monkey colony established at the Primate Research Institute (PRI), Inuyama, Japan, in mid-1970s currently consists of 16 subjects, among which 12 belong to *Aotus azarae* species. Among these, the

 

**Table 1** A select list of studies on longevous non-human primates[1]

| Primate[2] | Number | Age range (years) | Study Focus | Ref |
|---|---|---|---|---|
| Apes | | | | |
| Chimpanzee[3] | 5 | 40–59 | Brain weight | [23] |
| Chimpanzee[3] | 7 | 40–48 | Reproductive function | [19] |
| Chimpanzee[3] | 1 | >40 | Bone mineral density | [21] |
| Chimpanzee[3] | 9 | >40 | Sociobehavioral manifestations | [25] |
| Chimpanzee[3] | 9 | 40 (mean) | Behavior | [5] |
| Lowland gorilla[4] | 1 | 44 | Senile plaques | [31] |
| Lowland gorilla[4] | 2 | *c.* 41 | Sexual behavior and estrus cycle | [2] |
| Siamang[5] | 1 | *c.* 40 | General report | [45] |
| Old World monkeys | | | | |
| Japanese macaque[6] | 1 | *c.* 40 | Skeleton | [49] |
| Crab-eating macaque[7] | 1 | >35 | Senile plaques | [40] |
| Rhesus macaque[8] | 29 | 30–37 | Age-related pathology | [52, 53] |
| Rhesus macaque[8] | 7 | 31–36 | Life span | [50] |
| Rhesus macaque[8] | 1 | 34 | Menopause | [56] |
| Rhesus macaque[8] | 2 | 31 | Hyperthyroidism | [7] |
| Rhesus macaque[8] | 3 | 31 | Behavior and pathology | [12, 35] |
| Rhesus macaque[8] | 10 | ≥30 | Serum dehydroepiandrosterone sulfate | [30] |
| Rhesus macaque[8] | 1 | >30 | Degenerative joint disease | [14] |
| Rhesus macaque[8] | 1 | >30 | Pathology | [32] |
| Assamese macaque[9] | 1 | >30 | Pathology | [32] |
| Baboon, hamadryas[10] | 5 | >30 | Aging | [33] |
| Baboon, hamadryas[10] | 7 | >30 | Pathology | [32] |
| Vervet monkey[11] | 1 | 30 | Aging | [33] |
| New World monkeys | | | | |
| Woolly monkey[12] | 2 | 30–31 | Reproductive function | [38] |
| Squirrel monkey[13] | 6 | 22–27 | β/A4 amyloid in brain | [57] |
| Squirrel monkey[13] | 1 | >20 | Cerebral tumor | [26] |
| Capuchin monkey[14] | 1 | >40 | General postmortem | [24] |
| Prosimians | | | | |
| Fat-tailed dwarf lemur[15] | 1 | 15 | Brain iron and lipofuscin | [17, 18] |
| Grey lesser mouse lemur[16] | 1 | 12 | Brain iron and lipofuscin | [17, 18] |
| Ring-tailed lemur[17] | 16 | 10–14 | Fecundity, birth seasonality | [43] |
| Ring-tailed lemur[17] | 5 | 13–22 | Hemosiderosis | [47] |
| Black lemur[18] | 6 | 11–25 | Hemosiderosis | [47] |
| Brown lemur[19] | 1 | 14 | Hemosiderosis | [47] |
| Ruffed lemur[20] | 2 | 11–13 | Hemosiderosis | [47] |
| Ruffed lemur[21] | 3 | 12–28 | Hemosiderosis | [47] |
| Potto[22] | 3 | 11–24 | Reproductivity, life span | [10, 11] |

[1]The arbitrarily fixed age levels for longevous status among non-human primate groups are, >40 yrs (apes), >30 yrs (Old World monkeys), >20 yrs (New World monkeys) and >10 years (Prosimians), based on previously reported longevity records in captivity [6, 27].
[2]Species names are as follows: [3]*Pan troglodytes*; [4]*Gorilla gorilla*; [5]*Hylobates (Symphalangus) syndactylus*; [6]*Macaca fuscata*; [7]*Macaca mulatta*; [8]*Macaca fascicularis*; [9]*Macaca assamensis*; [10]*Papio hamadryas*; [11]*Chlorocebus(Cercopithecus) aethiops*; [12]*Lagothrix lagotricha*; [13]*Saimiri sciureus*; [14]*Cebus apella*, [15]*Cheirogaleus medius*; [16]*Microcebus murinus*; [17]*Lemur catta*; [18]*Lemur macaco macaco*; [19]*Lemur fulvus*; [20]*Variecia variegata variegata*; [21]*Variecia variegata rubra*; [22]*Perodicticus potto*.

oldest member was wild born and has passed 28 years in captivity, as of September 2005. Although the owl monkey colony at our facility has been in existence for three decades, partly due to specific and focused interests of most primatologists in Japan and partly due to the labor needed to develop non-invasive protocols which satisfy the primate care protocol adopted by our Institute since 1980s, these Neotropical monkeys barely received research attention. However, the members of this owl monkey colony had received routine veterinary care and none of the living members had suffered from any maladies including pain and were not in need of specific clinical veterinary care, medications for alleviating maladies and medical interventions. Until 2002, only two short reports were published based on the genetic [29] and circadian


J Med Primatol **35** (2006) 321–330 

activity rhythm [51] data collected from few selected members of this colony.

To remedy the then prevailing situation, we initiated our behavioral research program on this owl monkey colony in 2002. Recently, we [48] have compared the total sleep time (TST) of four members of this owl monkey colony, including the wild born oldest member Aa 23. Since in the wild, the young individuals of owl monkey disperse from the family group at the age of 3 years [59], we deduced that the oldest individual Aa 23 in our colony has already reached 30 years. According to the available published reports, and to our knowledge, this monkey thus appears to be the longest-lived owl monkey in captivity. As published data on longevous owl monkeys are scarce, our objectives for this study were (1) to prospectively quantitate the sleep of a longevous owl monkey longitudinally for 2 years, and (2) to evaluate the aging-induced change in spinal curvature.

## Materials and methods

### Animals

Three healthy female owl monkeys (*A. azarae*), sharing kinship, were used. The wild-born Aa 23 was identified as a longevous individual. Its offspring Aa 34 was used as the first control subject. At the commencement of the study in June 2003, the ages of Aa 23 and Aa 34 were >26 and 15 years respectively. In April 2004, Aa 34 gave birth to its ninth progeny Aa 56. Thus Aa 56 (grandprogeny of Aa 23) was also included as the second control subject, for the radiographic measurements in July 2005 towards the completion of the study. When radiographic measurements were taken, Aa 23, Aa 34 and Aa 56 weighed 1.30, 1.08 and 0.78 kg respectively. During the experimental period, while Aa 23 was housed in an individual stainless steel cage (100 × 70 × 60 cm), Aa 34 and its new-born progeny Aa 56 shared an adjacent cage of equal dimensions, since June 2005. Prior to that, Aa 34 was pair housed with its male partner and the newborn offspring, to accommodate the paternal care needs of the baby [59]. The cage dimensions in our facility for individuals and family group of four are in compliance with the required minimum space for this primate (of 1 kg mean weight) as defined by the US Animal Welfare Act 1992 [15, 16].

The colony room was maintained on a reverse, alternating 12 hours light (23:00–11:00 hours; 200 lx): 12 hours dark (11:00–23:00 hours; 0.01–0.5 lx) cycle. Lighting condition of the room was routinely checked by an illuminance meter (TopCon IM-5; Irie Seisakusho Ltd., Tokyo, Japan). Food and water were available to the monkeys *ad libitum*, and commercial pellet diet for New World monkeys (25.1 g protein and 10.6 g lipid/100 g diet) was supplemented daily with fresh fruits and twice-weekly with meal worms. Prior approval from the Research Committee of the Primate Research Institute for the reported experiments was obtained.

### Actigraphy

The sleep quantitation was carried out by an actiwatch (AW 64 model-MINIMITTER; Mini Mitter Company, Bend, OR, USA; containing 64 KB of on-board memory). Following anesthesia with ketamine HCl (10 mg/kg body wt; Sankyo, Tokyo, Japan), the AW (weighing 17 g), pre-set to collect activity–rest data of individual monkey with a sampling rate of 32 Hz and a sampling epoch of 1 minute, was suspended in an elastic band, and positioned on monkey's neck. For each subject, longitudinal data on activity pattern, TST and sleep episode length (SEL) were collected for 13 consecutive days, before removal of AW from monkey's neck. The accumulated data were retrieved into the computer, via Mini Mitter Actiwatch Reader through an RS-232 Serial Port and Activity Sleep Activity Monitoring Software, version 3.3 [37]. The definitions of the three activity–rest (sleep) parameters, as per manufacturer's instructions [37], are as follows:

1 Activity count: an arbitrary unit quantitating primate activity, computed from any omni-directional motion made by the caged monkey with a minimal resultant force of 10 mg. The instrument tallied the activity movements with reference to degree and speed of motion and converted these parameters to produce an electrical current that varied in magnitude. This derived algorithm is referred to as AW activity count, which is instrument specific; as of now, activity counts are incompatible for comparison with AWs from different commercial suppliers [36, 37]. Though AW activity count is thus an arbitrary unit and not suitable for determining the absolute activity of the animal in concrete terms, it can be usefully employed for evaluating comparative activity patterns among the monkeys wearing the AWs from the same commercial supplier.

2 TST: The cumulative amount of time measured in minutes in a continuous 24 hours circadian cycle (12 hours light phase:12 hours dark phase), that was scored as sleep. According to the Actiware–Sleep algorithm, based on 1 minute sampling epoch, activity counts of 40 or above were recorded as a wake epoch, and activity counts below this threshold value were recorded as a sleep epoch.

3 SEL: The mean length of blocks of continuous sleep, measured in minutes, falling between two wake bouts, in a 12 hours light phase of the 24 hours circadian cycle. The 12 hours light phase was preferred to measure this parameter, as owl monkeys predominantly rest during the light phase and not in the dark phase.

### Radiography

Radiographs of the whole body of the monkeys were taken to evaluate the alteration in spinal curvature as a consequence of aging. After anesthesia with ketamine HCl, as noted above, each subject was positioned (a) left lateral recumbently, and (b) dorso-ventrally, above the film cassette containing Fuji medical x-ray film 'RX-U' (Fujifilm Medical Co., Ltd. Tokyo, Japan). Care was taken to avoid overextension or flexion of limbs while the animals were positioned on radiographic cassette. The optimum X-ray exposure (Hitachi Medico portable X-ray machine) was 60 kV (20 mA) with exposure time set between 0.1 and 0.2 s. The distance between the film and X-ray beam source was 1 m. The films were wet processed at 20°C.

Spinal curvature of the monkeys was determined from the whole body radiographs, using kyphotic index (KI) as the criterion [34]. KI, calculated directly from the radiographs, is the ratio of AB/CD, where AB = length of the line marking the distance from seventh cervical vertebra to the sacral promontory and CD = the distance from AB to anterior border of the vertebral body that is furthest from AB [34].

## Results

### Activity–sleep quantitation

The daily activity levels, measured as mean AW activity counts, of the focal subject Aa 23 and its female offspring Aa 34 are shown in Fig. 1A. The daily mean (±SD) AW activity counts for the focal subject Aa 23 in June 2003, January 2004, January 2005 and May 2005 were 53 ± 7, 67 ± 10, 43 ± 16 and 44 ± 20 respectively. In comparison, the daily mean (±SD) AW activity counts for Aa 34 in August 2003, January 2004, June 2004 and June 2005 were 117 ± 30, 134 ± 30, 127 ± 20 and 97 ± 30 respectively. As expected, in all four data points spanning 2 years, the intensity of daily activity of aged Aa 23 monkey was almost one half or less to that of its progeny Aa 34. The AW activity count of Aa 56, the grandprogeny of Aa 23, was also determined in April 2005, when it reached 1 year. The daily mean (±SD) AW activity count of 323 ± 104 for Aa 56 (data not included in Fig. 1A) was nearly threefold higher to that of its female parent Aa 34, though it shared the same cage. We also positively ascertained from comparative individual videotape records of 24 hours duration of all

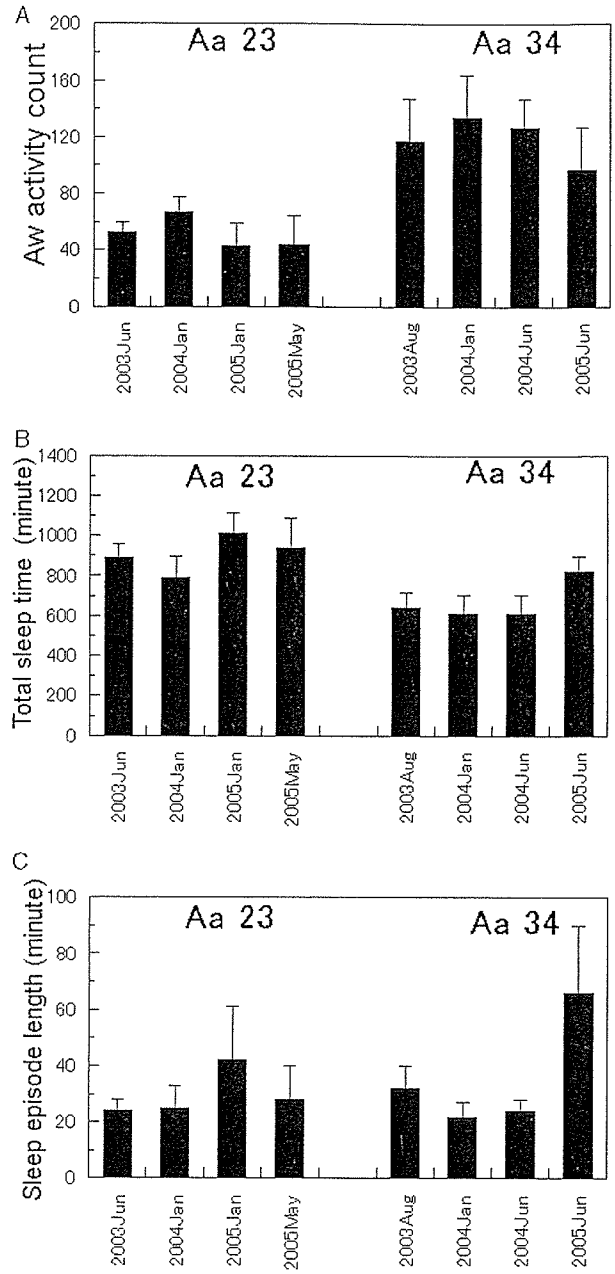


**Fig. 1** Comparison of measured activity and sleep parameters of longevous owl monkey (Aa23, aged >26 years) and its progeny (Aa 34, aged 16 years). (A) Activity counts, (B) total sleep time, and (C) sleep episode length. Each histogram represents the activity–sleep quantitation of consecutive 13 days. Results are expressed as daily mean ± SD.



J Med Primatol 35 (2006) 321–330 